UCRL-TR-202393

LAWRENCE LIVERMORE NATIONAL LABORATORY

Update of ENDL U(n,2n), U(n,γ), U(n,f) Evaluations

D. A. Brown, D. P. McNabb, B. Beck

18 February 2004

This document was prepared as an account of work sponsored by an agency of the United States Government. Neither the United States Government nor the University of California nor any of their employees, makes any warranty, express or implied, or assumes any legal liability or responsibility for the accuracy, completeness, or usefulness of any information, apparatus, product, or process disclosed, or represents that its use would not infringe privately owned rights. Reference herein to any specific commercial product, process, or service by trade name, trademark, manufacturer, or otherwise, does not necessarily constitute or imply its endorsement, recommendation, or favoring by the United States Government or the University of California. The views and opinions of authors expressed herein do not necessarily state or reflect those of the United States Government or the University of California, and shall not be used for advertising or product endorsement purposes.

This work was performed under the auspices of the U.S. Department of Energy by University of California, Lawrence Livermore National Laboratory under Contract W-7405-Eng-48.

Update of ENDL U$(n, 2n)$, U(n, γ), U(n, f) Evaluations

David Brown, Dennis McNabb, and Bret Beck
Lawrence Livermore National Laboratory, Livermore, CA 94550 USA
(Dated: February 18, 2004)

We are in the of re-evaluating all of the actinide cross section evaluations in LLNL's ENDL database, starting with uranium and focusing on inventory changing reactions. This article describes our first serious pass at updating the uranium cross section data, including estimates of cross section uncertainties. Futhermore, we are developing new tools to automate the re-evaluation and this article contains some preliminary results from these codes, namely the ^{235}U$(n, 2n)$ and ^{238}U$(n, 2n)$ evaluations.

I. INTRODUCTION

DNT has requested re-evaluations of the $(n, 2n)$, (n, γ), and (n, f) cross sections and uncertainties for all actinides, beginnning with the uranium isotopes A=230-241. The last ENDL release was in 1999 and it was only a partial update of the last major release which occured in 1994. Since then, there has been much progess in our understanding of reactions on actinides in general and on uranium in particular. This report details our determination of the best cross section evaluations and the insertion of these cross sections into the ENDL99 database. Our goal is two-fold: (1) produce the *best* cross section evaluations from existing databases – even if they significantly change the ENDL99 cross sections and (2) provide estimates of the uncertainties of the cross sections for each reaction. This effort begins with the uranium isotopes, but will eventually extent to all actinides and are the first in a series of modifications that will lead to the next ENDL database release.

In the past few years, there has been considerable effort in updating actinide cross section data and these efforts have resulted in updates to the JENDL3.3 [1] and ENDFB-VI [2] databases. We would like to capitalize on these efforts and adopt the best of these evaluations whereever possible. However, choosing the best evaluation must be done on a case by case basis. For several isotopes (e.g. ^{235}U and ^{238}U), there is plenty of data and recent evaluations are excellent representations of the cross sections. However in many cases, the there is no data to guide the evaluations (these reactions are ^{232}U(n, γ), ^{234}U(n, γ), ^{239}U(n, γ), all $(n, 2n)$ except ^{235}U$(n, 2n)$ and ^{238}U$(n, 2n)$, and all reactions on ^{240}U and ^{241}U). In these cases we must make our best guess as to the "best" evaluation and our estimates of the uncertainty must reflect this. Finally, many of the isotopes fall in between these two extremes, in which case one reaction may be handled either by fitting the data or taking an evaluation in which the fit was already done, while another reaction must be modeled. In two cases, ^{230}U and ^{231}U, there is no experimental data and insufficient information on the nuclei to model the reactions, so we restrict our range of interest to A=232-241 in this work.

We will use the `fudge` [4] package to perform these updates. First, `fudge` allows us to manipulate cross section data and obey cross section sum rules simultaneously. Second, it has a variety of cross section table manipulation functions that make transforming the data simple. Finally, it automates the production of grouped and processed nuclear data for use in downstream codes.

The uncertainty estimates are determined also on case by case basis. In the newest evaluations, there are now uncertainty estimates, but our ENDFB-VI to ENDL99 translation code `fete` [5] does not yet support them. So, lacking a simple way to extract this information from the evaluations, in these cases we will have to estimate them either using our fitter code `da_fit` [6] or by examining the data directly. In many other cases, there is little or no data to guide either the evaluators or our fits. In these cases, the evaluations are based on compound nuclear reaction modeling and we estimate the uncertainty from the uncertainties in the quantities input into the reaction models. These estimates are discussed within the text and they are particularly flawed for multi-step fission. However in this case, the relative uncertainty approaches the maximal relative uncertainty of 33% so we believe that more detailed investigation is not needed.

The updates in this work are not full re-evaluations so we must state what caveats should be recognized when using this work. First, we only updated the fission, $(n, 2n)$, capture, and total cross sections. In principal we should have updated also the elastic and (n, n')cross sections to account for the changes we made in other channels. Second, we did not have access to some of the most recent data (e.g. recent $^{U}238(n, 2n)$data from LANL) and we did not do a thorough investigation of the data we did use. Thus, the uncertainties stated here are likely smaller than they should be since we took the quoted uncertainties at face value. Finally, we do not have the resources to do a thorough investigation of the quality of the data in the resonance regions of the evaluations. We can however take what appears to be best representation of the resonance region based on our best judgement. We make special note of the cases where there is serious differences between evaluations or where there is no data to support detailed fits of resonances (so the evaluators chose to represent the resonance region as a picket fence of "average" resonances).

Before discussing each isotope, we detail some of the issues common to them all. This includes a discussion of the sum rules obeyed by the cross sections and a discus-

sion on how we treat the resonance region. In each isotope, we present plots of the capture, fission and $(n, 2n)$ cross sections. The capture cross sections are always presented on a log-log plot due to the large range in cross section values. The fission cross section is plotted both on a log-log scale and a linear scale, so that one can see both the overall shape of the cross section and see the absolute size of the cross section. The $(n, 2n)$ cross sections are always on a linear scale. In addition to these plots, we present a table of our uncertainty estimates, broken down by energy range. These estimates are not included in the ENDL database accompanying this document since the current version of the ENDL format does not support them. We also updated the total cross section data, although we do not discuss it in the text. Additionally, whenever apprioriate, we comment on the effect of our changes on other quantities such as the elastic cross section and the inelastic cross sections.

II. PRELIMINARIES

Before discussing the evaluations, we need to discuss some details common to most or all of the evaluations. First, we describe some sum rules that all of our cross section evaluations must obey. Second, we detail some general features of the optical model observables that underlie the evaluations. Finally, we detail how we do the uncertainty analysis for modeled cross sections.

A. Sum Rules

The cross sections for a projectile interacting with a nucleus are coupled through a few important sum rules. Some are a direct result of unitarity, while others are predictions of various reaction models. For our purposes, the relevant ones are pictured schematically in Fig. 1. In this section, we will concentrate on the interplay of the optical model and compound nuclear sum rules.

The first sum rule we consider is that imposed by the optical model. In a practical sense, the optical model is nothing more than the optical model potential (OMP) – the phenomenological interaction potential between the nucleus target and the (probably neutron) projectile. The OMP is both complex, allowing for absorption of the projectile by the nucleus, and has a bombarding energy dependence, an artifact of the removal of the nonlocality of the interaction potential. Working through the quantum mechanical scattering problem leads to a simple breakdown of the total cross section into two components: the shape elastic part and the absorption part. The shape elastic part is the cross section for scattering back into the original state through the optical model potential; the absorption part is the essentially cross section for doing anything else.

A compound nucleus is formed when a projectile is absorbed by a nucleus and the resulting excited nucleus equilibrates (forgetting the formation channel) and subsequently decays. Compound nuclear reactions predominate at energies < 20 MeV. The absorption cross section is a sum over all compound nucleus cross sections so it obeys the sum rule:

$$\sigma_{\text{abs}} = \sigma_{\text{CE}} + \sigma_{\text{f}} + \sigma_{\gamma} + \sigma_{(n,n')} + \sigma_{(n,2n)} + \ldots \quad (1)$$

In general, the branching ratios between channels can generally be modeled statistically. However, we do not have a complete understanding of compound nucleus decay through fission so the branching ratio to fission is a large source of theoretical uncertainty in this expression. Experimentally, the fission cross section has a unique signature so is straightforward to measure even though the fission fragments often obscure the signals from competing reactions.

The compound elastic cross section, σ_{CE}, is the cross section for forming a compound nucleus, then the nucleus decaying back into the original state. Thus, it has the energy balance of an elastic scattering, but the angular dependence of a compound nucleus reaction. The elastic cross section is a combination of the two:

$$\sigma_{\text{elas}} = \sigma_{\text{CE}} + \sigma_{\text{SE}} \quad (2)$$

This coupling between the OMP derived shape elastic and the compound elastic cross sections implies that if we alter the fission cross section, then to keep the absorption cross section fixed (since it is constrained by the optical model), we must adjust not only the capture, (n, n') and $(n, 2n)$ cross sections, but also the compound elastic and hence the elastic cross section.

Combining the optical model and compound nuclear sum rules leads us to a requirement that the various cross sections add up properly:

$$\sigma_{\text{non-elas}} = \sigma_{\text{f}} + \sigma_{\gamma} + \sigma_{(n,n')} + \sigma_{(n,2n)} + \ldots \quad (3)$$

and

$$\sigma_{\text{tot}} = \sigma_{\text{elas}} + \sigma_{\text{non-elas}} \quad (4)$$

B. Optical Model Predictions

In this work, we are considering 10 separate actinides with at least 3 separate OMP's underlying the various evaluations. Given this and the fact that we are to provide uncertainty estimates on the cross sections we produce, we need to discuss the OMP and their predictions in some detail.

The OMP is usually constrained by measurements of the total cross section and angular distributions from the elastic scattering. Since it is often straight-forward to measure the total cross section it is often possible to produce very high quality OMP's and hence predict the absorption and shape elastic cross sections. Furthermore, we can compute the transmission coefficients that are an

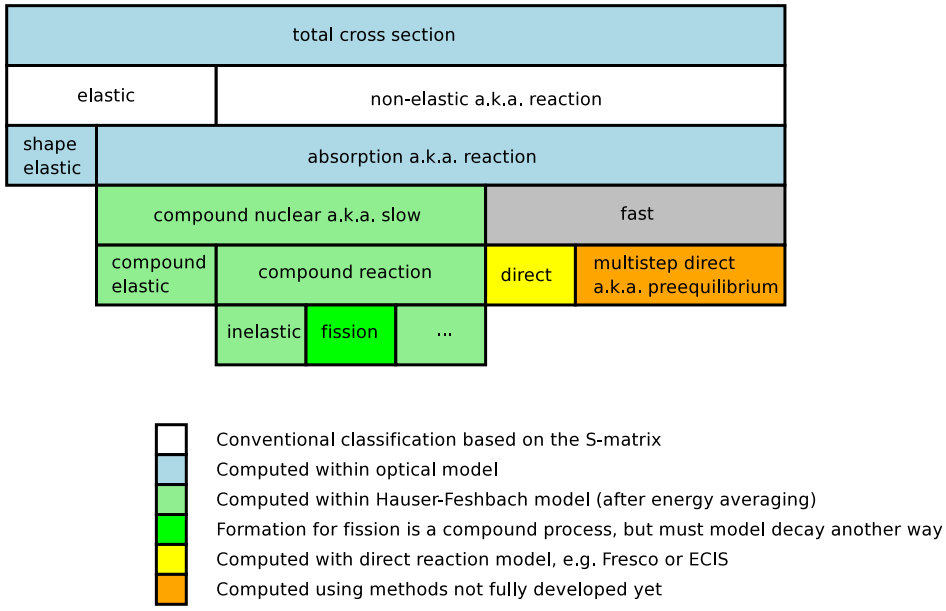

FIG. 1: Cartoon explaining the sum rules that apply to the various cross section data.

important input for compound nuclear reactions using these OMP's.

In Fig. 2, we plot the evaluated total cross section for all of the uranium isotopes of interest as evaluated by LANL in Refs. [2, 9, 14]. In this figure, we see that the evaluated cross sections do not vary much from isotope to isotope over this energy range. This is despite the expected changes in deformation and the known $A^{2/3}$ variation of the optical model cross section. Given this, we can take the spread in the evaluated cross sections as an estimate of the uncertainty on the total cross section in the optical model calculations. The lower panel in Fig. 2 shows this relative uncertainty.

The total, absorption and shape elastic cross sections as well as the transmission coefficients (for particle exit channels) used in compound nuclear model cross sections are all related to the S-matrix (which is itself modeled in the optical model):

$$\sigma_{\rm tot} = \frac{2\pi}{k^2}\sum_\ell \left[(\ell+1)(1-{\rm Re}S_\ell^+) + \ell(1-{\rm Re}S_\ell^-)\right] \quad (5)$$

$$\sigma_{\rm abs} = \frac{\pi}{k^2}\sum_\ell \left[(\ell+1)(1-|S_\ell^+|^2) + \ell(1-|S_\ell^-|^2)\right] \quad (6)$$

$$\sigma_{\rm SE} = \frac{\pi}{k^2}\sum_\ell \left[(\ell+1)|1-S_\ell^+|^2 + \ell|1-S_\ell^-|^2\right] \quad (7)$$

$$T_\ell = 1-|S_\ell^\pm|^2 \quad (8)$$

Since the total cross section goes like one power of the S-matrix and the other parameters go like the S-matrix squared, we can expect that the relative uncertainties on these parameters is controlled by the uncertainty on the total cross section. Roughly speaking, we take:

$$\frac{\delta\sigma_{\rm abs}}{\sigma_{\rm abs}}, \frac{\delta\sigma_{\rm SE}}{\sigma_{\rm SE}}, \frac{\delta T_\ell}{T_\ell} \sim 2\frac{\delta\sigma_{\rm tot}}{\sigma_{\rm tot}} \quad (9)$$

In this work, we will often need the shape elastic cross section in order to ensure that the sum rules are obeyed correctly. Since the shape elastic cross section is predicted by the optical model and since the OMP varies only weakly in the mass range considered here, we may us the same shape elastic cross section for all nuclei, as needed. The shape elastic cross section that we use is plotted in Fig. 3 and is a result of an `ecis` calculation performed by Young and Chadwick [9] using a deformed optical model tuned for this mass region.

C. Uncertainties on Modeled Cross Sections

For several evaluations, there is no data and the cross section must be modeled. In all of the cases here, this modeling is performed with a compound nucleus reaction model (usually `gnash`). In such models, a single-step reaction is given by

$$\sigma_i \sim \sigma_{\rm abs}\frac{\Gamma_i}{\sum_j \Gamma_j} \quad (10)$$

where Γ_i is the partial width for decaying into channel i. Hence ${\rm BR}_i = \Gamma_i/\sum_j \Gamma_j$ is the branching fraction into channel i. Similarly, the $(n,2n)$ cross section (the only two-step reaction we consider) is given by

$$\sigma_{(n,2n)} \sim \sigma_{\rm abs}\frac{\Gamma_n^{A+1}}{\sum_j \Gamma_j^{A+1}}\frac{\Gamma_n^{A}}{\sum_j \Gamma_j^{A}} = \sigma_{\rm abs}{\rm BR}_n^{A+1}{\rm BR}_n^{A} \quad (11)$$

Here we have added the total nucleon number A as an index to remind ourselves which compound nucleus is relevant for each stage.

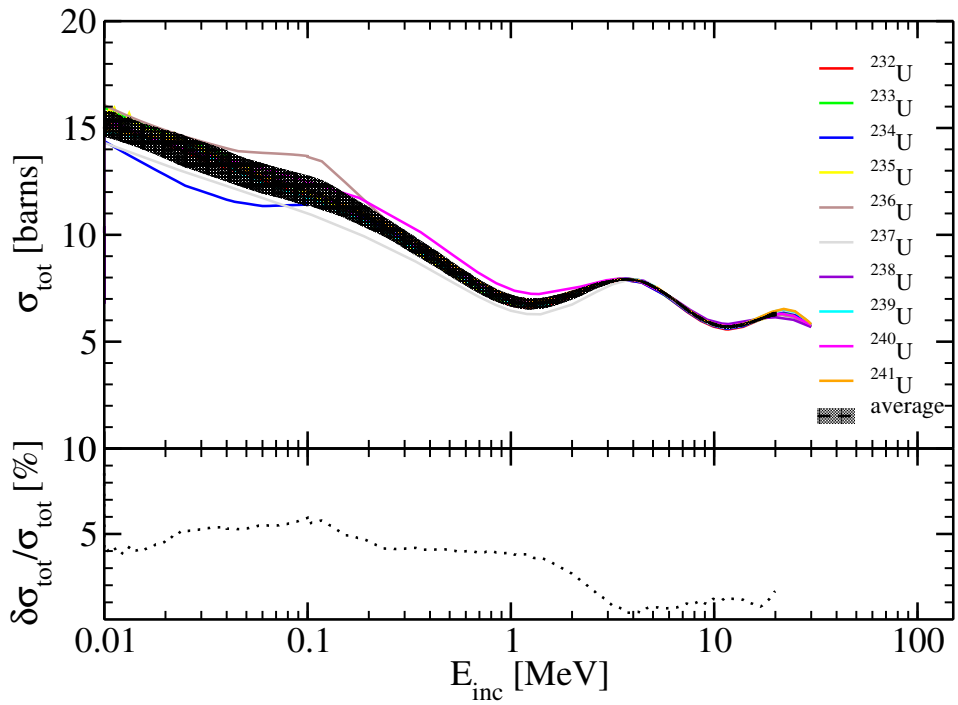

FIG. 2: The total cross section for each uranium isotope from the LANL evaluations. The lower panel shows the relative spread in the total cross sections.

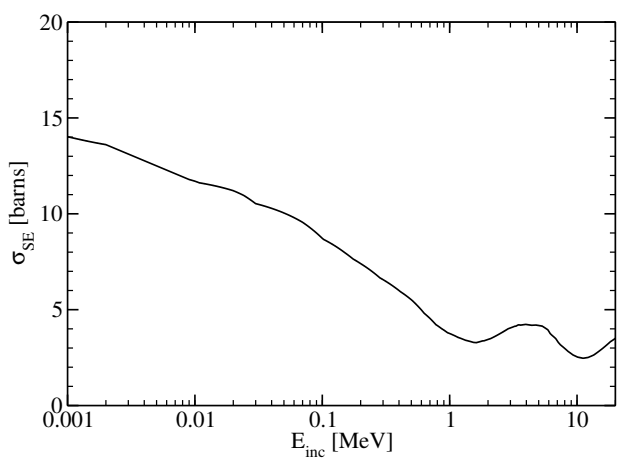

FIG. 3: The shape elastic cross section used in this work.

In either case, the uncertainty on the absorption cross section is given by the optical model as discussed above. The partial widths are given by

$$\Gamma_i^A(E) \sim \int_0^{E-E_{\rm sep}} d\epsilon T_i(\epsilon)\rho^A(E-E_{\rm sep}-\epsilon) \qquad (12)$$

Here $E_{\rm sep}$ is the separation energy for this channel, T_i is the transmission coefficient for this channel and ρ is the level density for this compound nucleus. Thus, we could estimate the relative uncertainty of the partial widths as

$$\frac{\delta\Gamma_i^A}{\Gamma_i^A} \sim \sqrt{\left(\frac{\delta T_i}{T_i}\right)^2 + \left(\frac{\delta\rho^A}{\rho^A}\right)^2} \qquad (13)$$

provided we can estimate the uncertainty in the level density.

In order to estimate the uncertainty on the level density, we note that typically $\rho(E) \sim \rho_0 e^{E/T}$. Thus, the cumulative level distribution, $N(E)$, is given roughly by

$$\begin{aligned} N(E) &= \int_0^{E_{\rm max}} dE\rho(E) \\ &\sim T(\rho(E_{\rm max}) - \rho(0)) \\ &\approx T\rho(E_{\rm max}) \end{aligned} \qquad (14)$$

Since we can count the cumulative level distribution directly by counting the levels in a given level scheme, we have an estimate of the level density. Furthermore, since $N(E)$'s uncertainty is $\delta N(E) = \sqrt{N(E)}$, we have a rough way to estimate the relative uncertainty on the level density:

$$\frac{\delta\rho(E)}{\rho(E)} \sim \frac{1}{\sqrt{N(E)}} \qquad (15)$$

Table I provides our estimate of the relative uncertainty of the level density for each uranium isotope of interest. In these calculations, we subtract off 20 levels since the low-lying levels typically do not obey the assumed exponential rise. This only increases the estimate of the the relative uncertainty in the level densities.

Isotope	No. known levels	No. added levels	$E_{\max}$ (MeV)	$N(E_{\max})$	$\delta N(E_{\max})$	$\delta\rho(E_{\max})/\rho(E_{\max})$
^{231}U	8	0	1.268	–	–	33%
^{232}U	32	0	2.660	12	3.46	29%
^{233}U	88	0	2.301	68	8.25	12%
^{234}U	151	15	4.297	146	12.1	8%
^{235}U	152	0	4.043	132	11.5	9%
^{236}U	109	0	5.077	89	9.43	11%
^{237}U	182	0	2.308	162	12.7	8%
^{238}U	153	0	5.513	133	11.5	9%
^{239}U	107	0	3.107	87	9.33	11%
^{240}U	14	0	2.010	–	–	33%
^{241}U	0	0	0	–	–	33%
^{242}U	0	0	0	–	–	33%

TABLE I: Estimates of level density uncertainty. 33% is the maximum uncertainty possible and is used where no other estimate is possible. The number of added levels are additional levels used in the ^{235}U$(n,2n)$ evaluation of Ref. [20].

Now let us combine these results to obtain the relative uncertainty on one-step and two-step compound nuclear cross sections. Under the assumption that the capture and fission channels have the same relative uncertainty as the particle exit channels, the uncertainty on the branching ratios is comparable to that of the partial widths: $\delta\mathrm{BR}_i/\ \mathrm{BR}_i \sim \delta\Gamma_i/\Gamma_i$. Strictly speaking the relative uncertainty on the partial widths is probably very different for the different channels, but lacking any better scheme we have made this crude assumption. In any event, with this approximation, the one-step and two-step compound cross sections have the following relative uncertainties:

$$\frac{\delta\sigma_{\text{1-step}}}{\sigma_{\text{1-step}}} \sim \sqrt{2\left(\frac{2\delta\sigma_{\text{tot}}}{\sigma_{\text{tot}}}\right)^2 + \left(\frac{\delta\rho^{A+1}}{\rho^{A+1}}\right)^2}$$
$$\frac{\delta\sigma_{(n,2n)}}{\sigma_{(n,2n)}} \sim \sqrt{3\left(\frac{2\delta\sigma_{\text{tot}}}{\sigma_{\text{tot}}}\right)^2 + \left(\frac{\delta\rho^{A+1}}{\rho^{A+1}}\right)^2 + \left(\frac{\delta\rho^{A}}{\rho^{A}}\right)^2} \tag{16}$$

In this framework, multi-step fission should also be treated as a two or more step reaction. In practice, we found that the uncertainty for modeled multi-step fission always approached the maximal 33% relative uncertainty (see the next paragraph) using Eq. (16) so we do not need a more detailed investigation.

In all cases, there are many sources of uncertainty in these cross sections so it is possible that we may arrive at a large model uncertainty. In these cases, we cap the relative uncertainty at 33% since this allows the modeled value to be consistent with zero at the 99% confidence level (corresponding to "3σ").

III. ^{232}U

This nuclide is not present in ENDL99, so we are faced with two tasks: determining the best fission, capture and $(n, 2n)$ evaluations and determining the outgoing particle distributions. Fortunately there is experimental data on the fission reaction that we can use as a guide. In the end our final evaluation is a patchwork of the JENDL3.3 evaluation [1] and a slightly modified LANL evaluation [9]. We discuss the modification below. The recent LANL evaluation itself is also a patchwork of the recent LANL work above 2 keV and an earlier ENDFB-VI evaluation below 2 keV. At 2 keV, there is a step where these two evaluations are pasted together. Since JENDL3.3 readjusted the smooth fission background of the fission cross section in order to agree better with experimental data in the resonance region we chose to do our own pasting. For fission, we use the JENDL3.3 cross section below 10 keV, we use the LANL cross section above 20 keV and in between we linearly interpolate. For capture, we use JENDL3.3 below 2 keV and LANL above 5 keV.

To deal with the outgoing particle distribution problem, we could do one of two things. We could substitute the ^{234}U distributions in for ^{232}U, changing the ENDL99 headers appropriately. Since both are even-even nuclei, this substitution is not unreasonable. Alternately, we could adopt the distributions from either the LANL or JENDL3.3 evaluations. We chose to use the LANL evaluation since it was generated with the `gnash` Hauser-Feshbach code so we can be guaranteed consistency between the various distributions and cross sections. JENDL3.3 used a similar code to generate the distributions, but using less complete nuclear structure input.

Most of the LANL evaluation is taken from `gnash` calculations. The main exception is the fission cross section which is taken from a fit to the existing fission data. The fact that the fission cross section is modified from the `gnash` results, while the rest of the cross sections remain unchanged means that the competition between the various channels may not be represented properly. We will return to this point when discussing the capture. To assess the uncertainty on this fission cross section itself, we look to the uncertainty on the data. In the energy range > 100 keV, the only trustworthy data come from Fursov [13] and below this range, the data mainly are from Farrell [12]. Above roughly 7 MeV, third chance fission turns on and the LANL evaluators chose to model the cross section using `gnash` . It is clear that the `gnash` calculations underestimate the 14 MeV data of Fursov *et al.*. However, we believe that this point is questionable for several reasons. This point is not mentioned in the documentation accompanying the data entry in the EXFOR database and the documentation suggests that the data stop at 7.4 MeV. We have not checked the original reference. More importantly, this data point exceeds the total absorption section making it inconsistent with the optical model value. Above 7 MeV, we use the `gnash` evaluation and compute uncertainty using Eq. (16). Our uncertainty estimates are collected in Table II.

Energy Range (MeV)	% Error Estimate		
	(n,γ)	(n,f)	$(n,2n)$
0.01-0.1	20	26	n/a
0.1-1.0	14	5.3	n/a
1.0-7.31	20	5.3	n/a
7.31-20.0	33	12	33

TABLE II: Error estimates for reactions on the ^{232}U nucleus.

The LANL $(n, 2n)$ cross section comes directly from their `gnash` calculation. Hauser-Feshbach calculations require several types of input to work: level schemes for the compound nuclei involved, level densities for the compound nuclei, gamma ray strength functions, and transmission coefficients. There is acceptable nuclear structure information for ^{232}U and ^{233}U to model transitions to the discrete levels. Both level densities and gamma ray strength functions can be gotten from systematics. The transmission coefficients are products of optical model calculations, so should be in good shape. The competition problem mentioned above is not an issue here because the `gnash` fission calculation is in good agreement with data above the $(n, 2n)$ threshold [9]. We use Eq. (16) to compute uncertainty here.

Our capture cross section is a modification of the one in the LANL evaluation. To understand why we modified it, consider the capture cross section in the Hauser-Feshbach model:

$$\sigma_\gamma \sim \sigma_{\rm abs} \frac{\Gamma_\gamma}{\Gamma_\gamma + \Gamma_f + \Gamma_{CE} + ...} \tag{17}$$

Here Γ_i is the width for going into channel i. If one of the widths is off, the others may be all right, but owing to competition, all of the reaction cross sections will be off. Of course if more then one reaction rates is off (which very well may be – the optical model potential, the level density and gamma ray strength function are all extrapolated to this nucleus), what is in the LANL evaluation is the best we can realistically do.

We believe that both the level density and the optical model potential are under control. The variation of the optical model potential with each nucleus is mainly due to the changing shape and size of each nucleus. In the actinides, this variation is a small fraction of the total nuclear size owing to the large A. Also, the level density is under control because it may be fit to the cumulative level distribution, which is well understood.

The remaining question is the gamma ray strength function. Young *et al.*. fix the normalization of the gamma ray strength function to reproduce the known ratio of the capture width to average level spacing, $2\pi\Gamma_\gamma/D_0$, when there is no experimental data and to trust the energy dependence of the (n, γ) gamma ray strength function in `gnash` . In the case of ^{232}U, we know

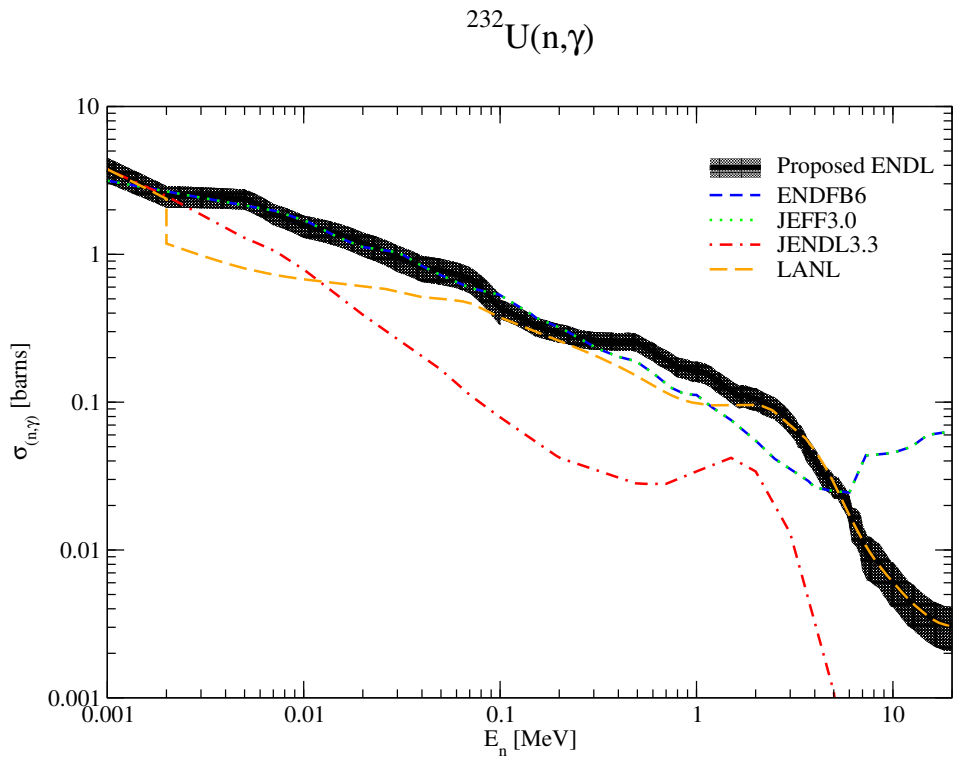

FIG. 4: The ^{232}U capture cross section. In this and all other figures, the ENDFB-VI evaluation is the blue short-dashed line, all LLNL evaluations are solid black lines, the JENDL3.3 evaluation is the red dot-dashed line, the JEFF3.0 evaluation is the green dotted line and the recent LANL evaluation is the orange long-dashed line.

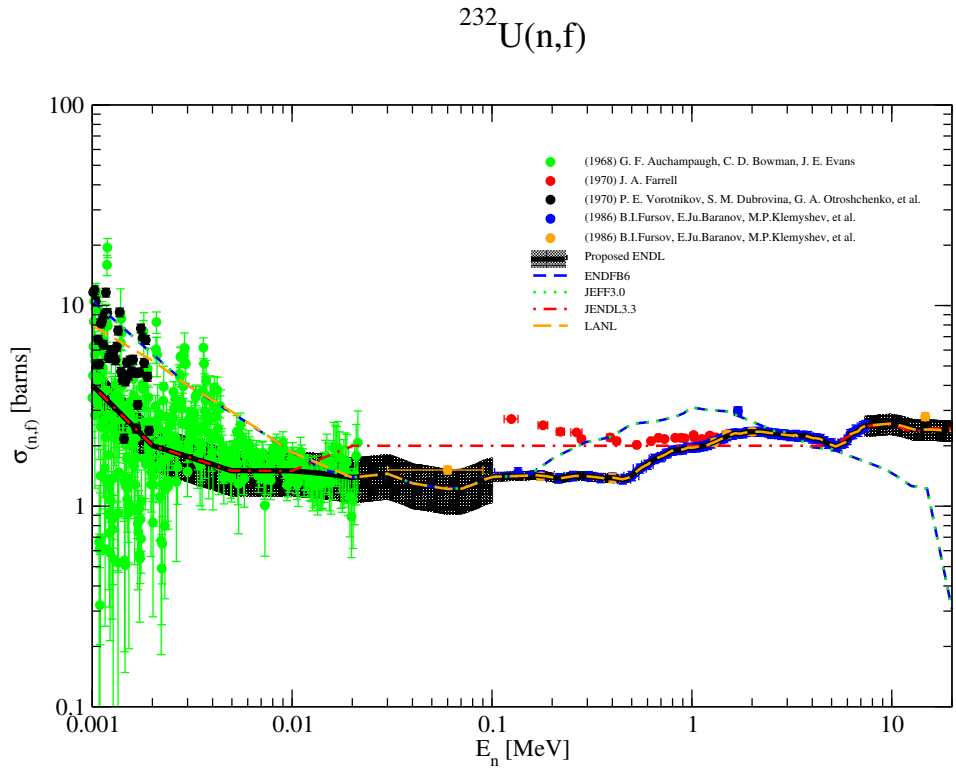

FIG. 5: The ^{232}U fission cross section on a logarithmic scale.

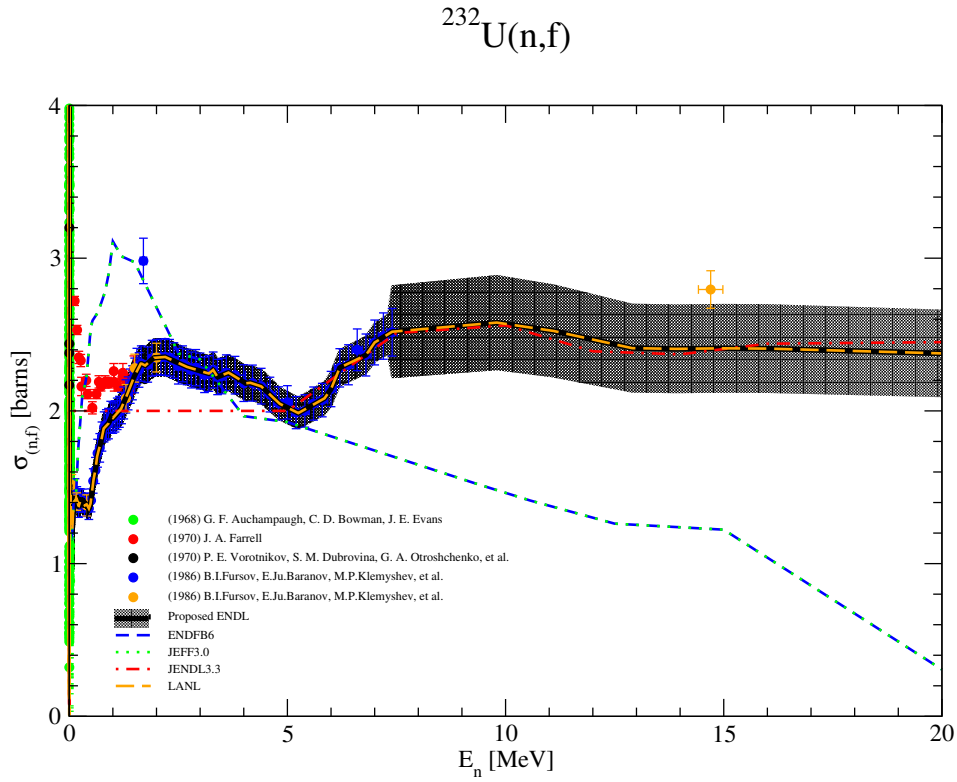

FIG. 6: The ^{232}U fission cross section on a linear scale.

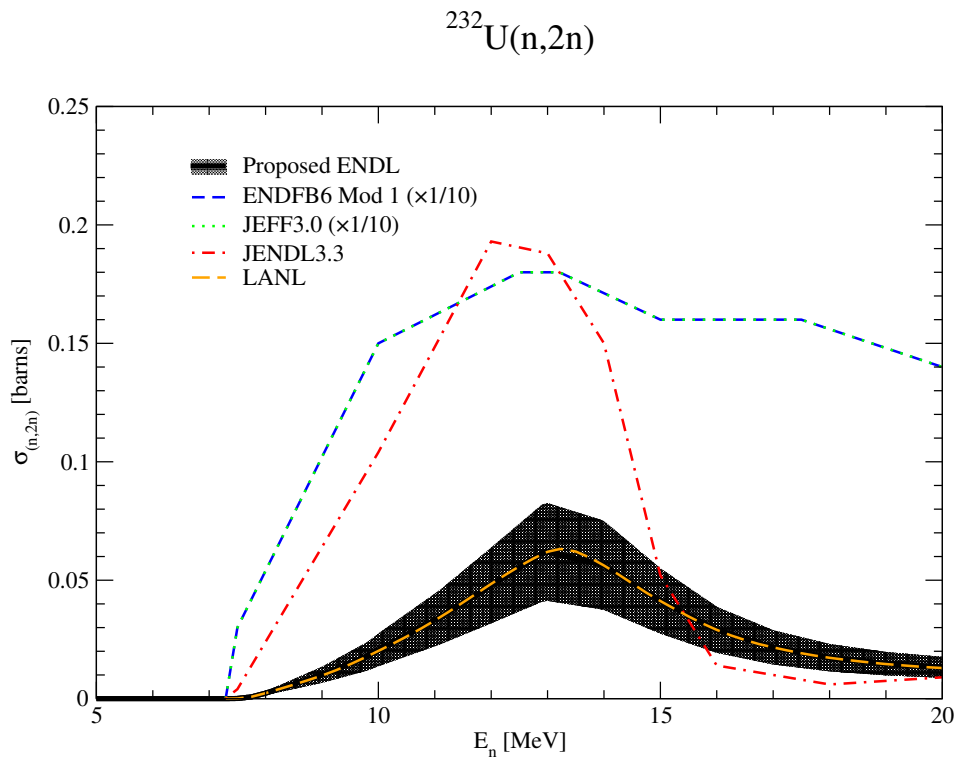

FIG. 7: The ^{232}U$(n, 2n)$ cross section.

D_0 but do not have Γ_γ. For this case, Young *et al.*infer a value from ^{234}U, ^{236}U, and ^{238}U.

Assuming that the parts of the LANL evaluation are fine, we can actually "replace" the bad Γ_f in (17) using the fit to the fission cross section used in the LANL evaluation and the original `gnash` calculations of Young *et al.* [11]. A little algebra shows that we can write a corrected cross section in terms of the corrected fission cross section and the uncorrected partial cross sections:

$$\sigma_x^{\text{fixed}} = \sigma_x^{\text{orig}} + \left(\sigma_f^{\text{orig}} - \sigma_f^{\text{fixed}}\right) \frac{\sigma_x^{\text{orig}}}{\sigma_{\text{CE}} + \sigma_\gamma + \sigma_{(n,n')} + ...} \tag{18}$$

The sum in the denominator here runs over all open channels. The rescaled capture cross section is shown in Fig. 4. The uncertainty resulting from the combination of this rescaling and previous modeling is given by:

$$\frac{\delta\sigma_x^{\text{fixed}}}{\sigma_x^{\text{fixed}}} \approx \sqrt{\left(\frac{\delta\sigma_x^{\text{orig}}}{\sigma_x^{\text{orig}}}\right)^2 + (\delta\sigma_f^{\text{fixed}})^2 \left(\frac{\sigma_x^{\text{orig}}/\sigma_x^{\text{fixed}}}{\sigma_{\text{CE}} + \sigma_\gamma + ...}\right)^2} \tag{19}$$

to leading order in the ratio $\sigma_x^{\text{orig}}/(\sigma_{\text{CE}}+\sigma_\gamma+\sigma_{(n,n')}+...)$. This uncertainty is shown in Table II and the uncertainty band in Fig. 4.

To complete the evaluation, we note that it is not enough to rescale the capture cross section. The competition problem affects all open channels below roughly 1 MeV. So, we should rescale the compound elastic and the (n, n') channels as well. We did not do this at this time but will revisit this problem in the next re-evaluation of these nuclei. As stated above, the $(n, 2n)$ and other higher energy channels are unaffected by this competition because the `gnash` calculation did an acceptable job of reproducing the fission cross section at higher energies.

Energy Range (MeV)	% Error Estimate		
	(n,γ)	(n,f)	$(n,2n)$
0.001-0.01	33	3.0	n/a
0.01-1.0	21	2.0	n/a
1.0-5.79	33	2.0	n/a
5.79-20.0	33	2.5	15

TABLE III: Error estimates for reactions on the ^{233}U nucleus.

IV. ^{233}U

We adopt much of the new LANL evaluation [14] for this nuclide, the exception being the new JENDL3.3 fission evaluation from Ref. [8]. The resonance parameters are taken directly from the LANL evaluation since they are taken from a new ORNL evaluation present in the newest ENDFB-VI evaluation. In all of the LANL evaluations, there is a step at 40 keV caused by patching the ORNL evaluation onto LANL evaluation. We smoothed this step by linearly interpolating both the fission and the elastic scattering cross sections from 36 - 44 keV. The evaluations we propose for the new ENDL release are shown in Figs. 8, 10, 9, and 11.

The LANL evaluation uses a combination of data fit and `gnash` calculations above the 40 keV pasting energy. The LANL evaluators went to great length to tune the `gnash` calculations to reproduce the fission (leaving an overall 5% difference between the model calculation and measurements), total, and elastic cross sections. This means there is no competition in this case. Thus, we can adopt the LANL $(n,2n)$, elastic, and capture cross sections directly and maintain overall consistency. We use Eq. (16) for the $(n,2n)$ uncertainties shown in Table III.

The capture uncertainty is taken directly from available data. In the range from 1 keV - 10 keV, we obtained the uncertainty from the standard deviation of the Weston data [16] since uncertainties are not given in the EXFOR data. In the range from 10 keV - 1 MeV, the uncertainty is obtained from the uncertainty on the measurement of Hopkins [15]. Finally, above 1 MeV, the evaluations all drop exponentially and the spread in the evaluations is quite large. Lacking any experimental data, we adopt the LANL values since the rest of the evaluation is consistent with data in this energy range, and since the evaluation is based on a `gnash` calculation, the capture cross section must be similarly reasonable. We set the uncertainty solely based on the modeling uncertainty in Eq. (16).

The fission cross section and uncertainty are both taken from the recent JENDL3.3 evaluation discussed in Ref. [8]. In that work, the authors performed a combined generalized least-square fit to the fission cross section and ratio measurements for several nuclei including ^{233}U. The ratio data they use is not shown in Figs. 9 or 10. While they did not apparently use all available data, their experimental database is quite large and sufficient to provide an excellent representation of the cross section. As a by product of their fitting, they obtain the fit uncertainties over the entire energy range of interest and these are reflected in Table III. As discussed in the LANL evaluation write-up [14], the LANL fission evaluation is in excellent agreement with the JENDL3.3 evaluation.

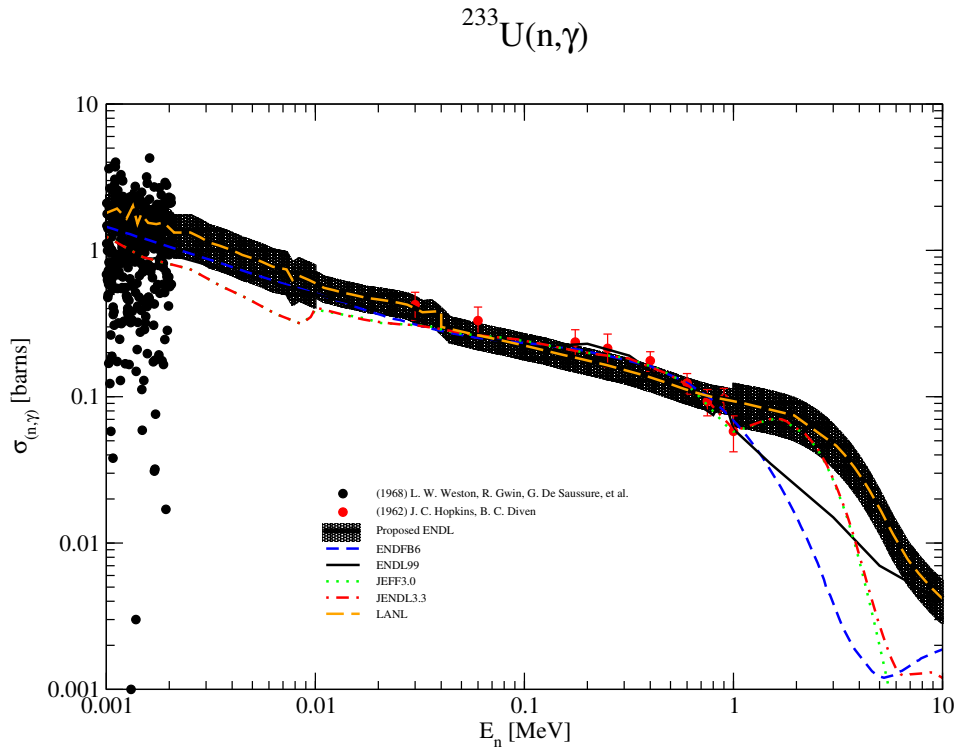

FIG. 8: The ^{233}U capture cross section.

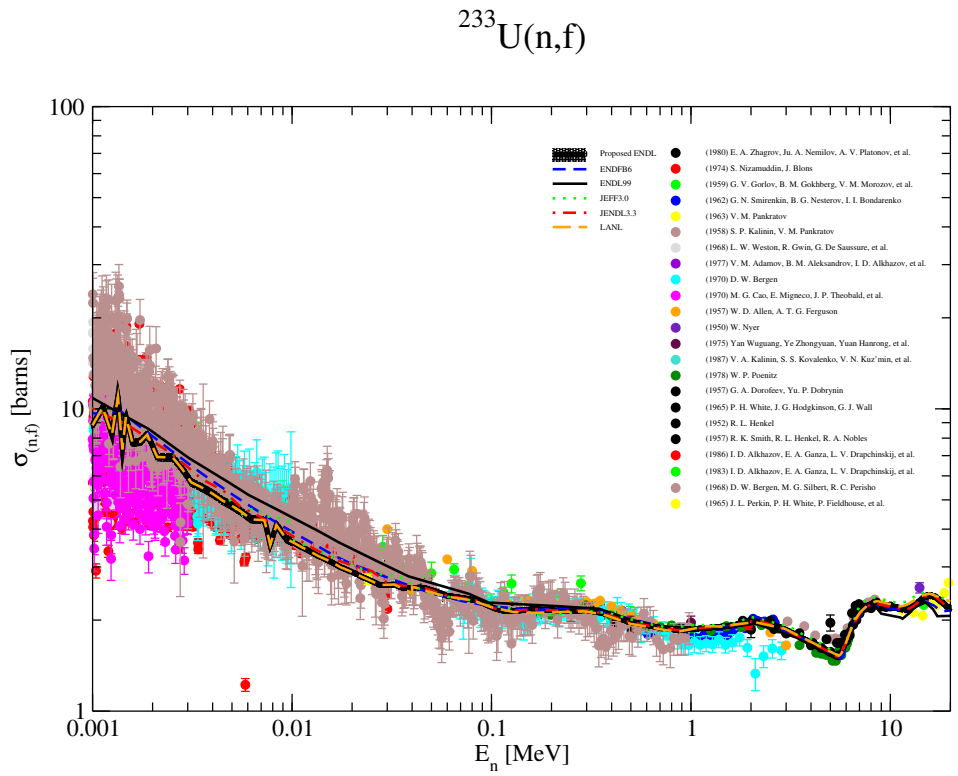

FIG. 9: The ^{233}U fission cross section on a logrithmic scale.

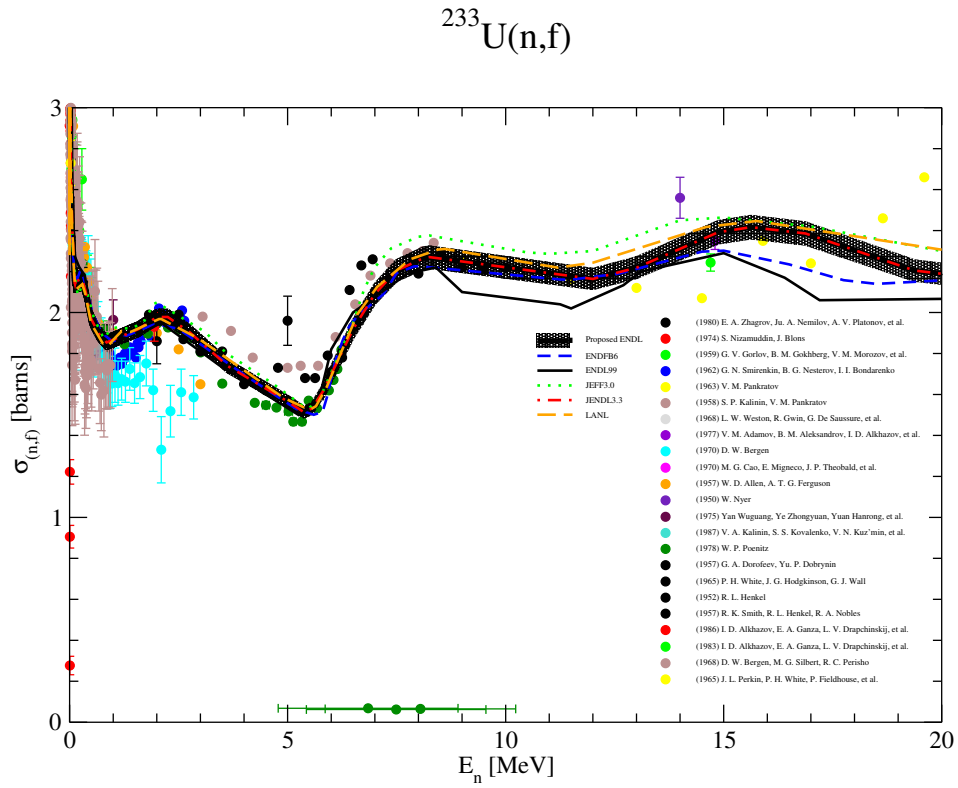

FIG. 10: The ^{233}U fission cross section on a linear scale.

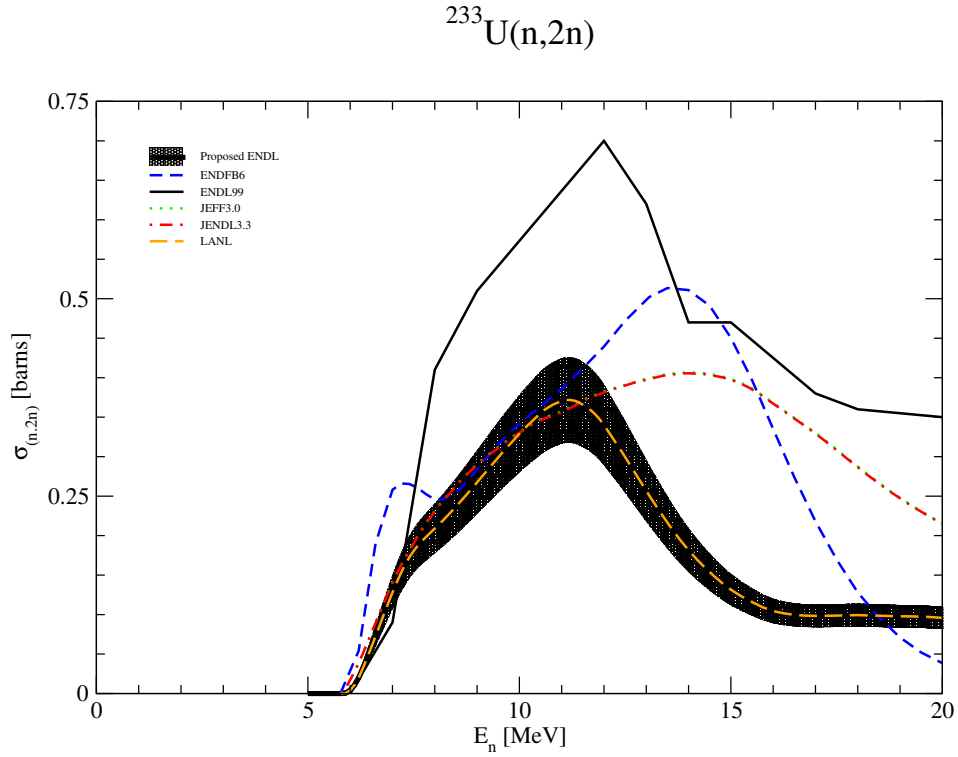

FIG. 11: The ^{233}U$(n, 2n)$ cross section.

Energy Range (MeV)	% Error Estimate		
	(n,γ)	(n,f)	$(n,2n)$
0.001-0.1	12	20	n/a
0.1-6.87	18	17	n/a
6.87-20.0	33	20	33

TABLE IV: Error estimates for reactions on the ^{234}U nucleus.

V. ^{234}U

Here we adopt the entire LANL evaluation, with only minor modifications. Our main changes are: we smoothed out the step at 100 keV where the LANL evaluators patched the low energy cross sections onto the high energy parts and we corrected the capture and $(n,2n)$cross sections for the competition problem seen above in ^{232}U.

The resonance region for all evaluations came from Ref. [17]. Both JENDL3.3 and LANL evaluations modify the resonance region to better agree with the $\langle\Gamma_\gamma\rangle$ in Ref. [10]. However, only LANL also accounts for the recent data of Muradyan *et al.* [18] so we adopt the LANL resonance region.

The LANL fission cross section is a fit to both the absolute measurements (shown in Figs. 14 and 13) as well as ratio data (not shown). We take the uncertainties as the average uncertainties of the data.

The $(n,2n)$, elastic and capture cross sections are taken directly from a `gnash` calculation. In principal, the LANL evaluations have the same competition problem mentioned above. However, ^{234}U is a threshold fissioner so that the change in fission cross section only becomes sizable above 500 keV, where the LANL fission model agrees with the data. Still, it is a problem, so we rescale the elastic and capture cross sections in the manner of ^{232}U. As before, we compute the modeling uncertainty using Eqs. (16) and (19) for the $(n,2n)$ and capture cross sections.

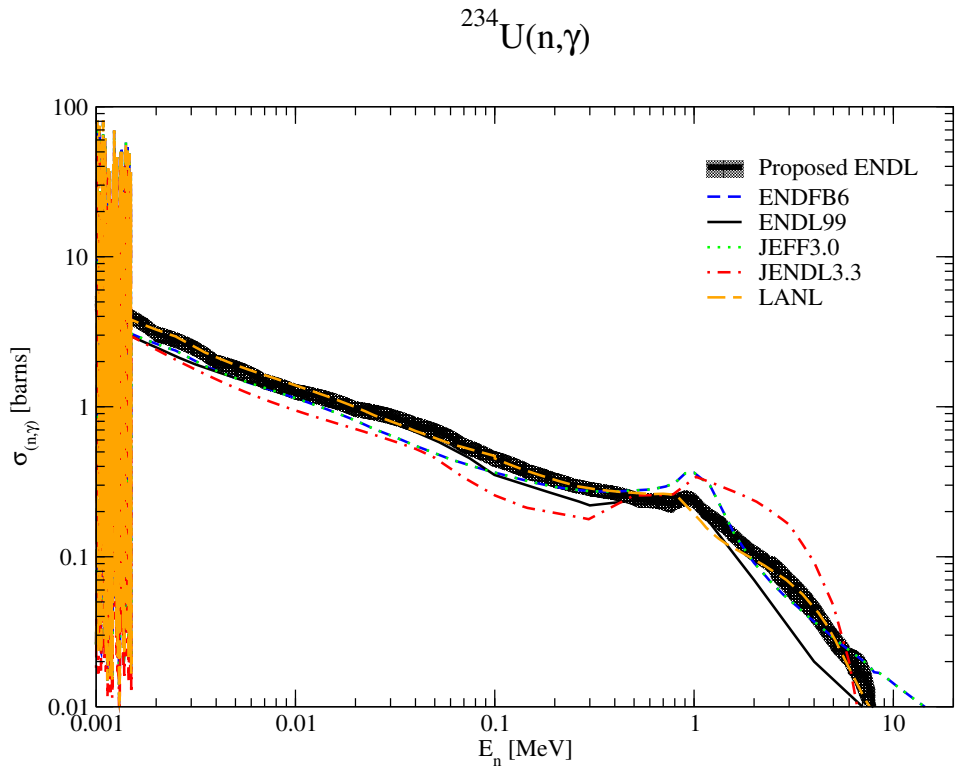

FIG. 12: The ^{234}U capture cross section.

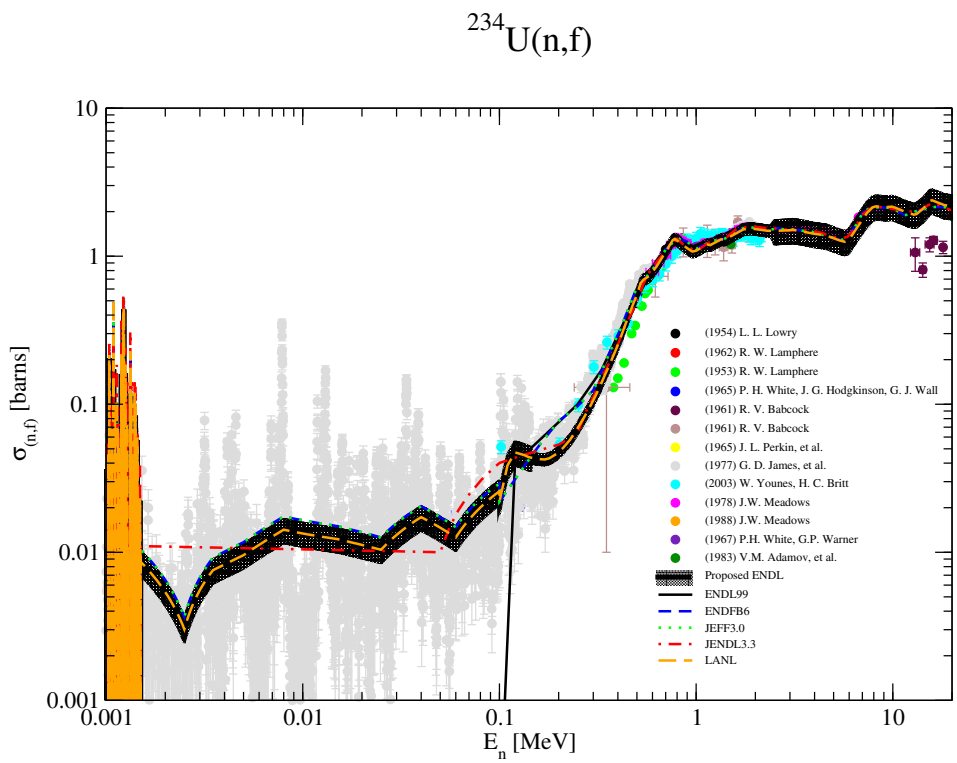

FIG. 13: The ^{234}U fission cross section on a logarithmic scale.

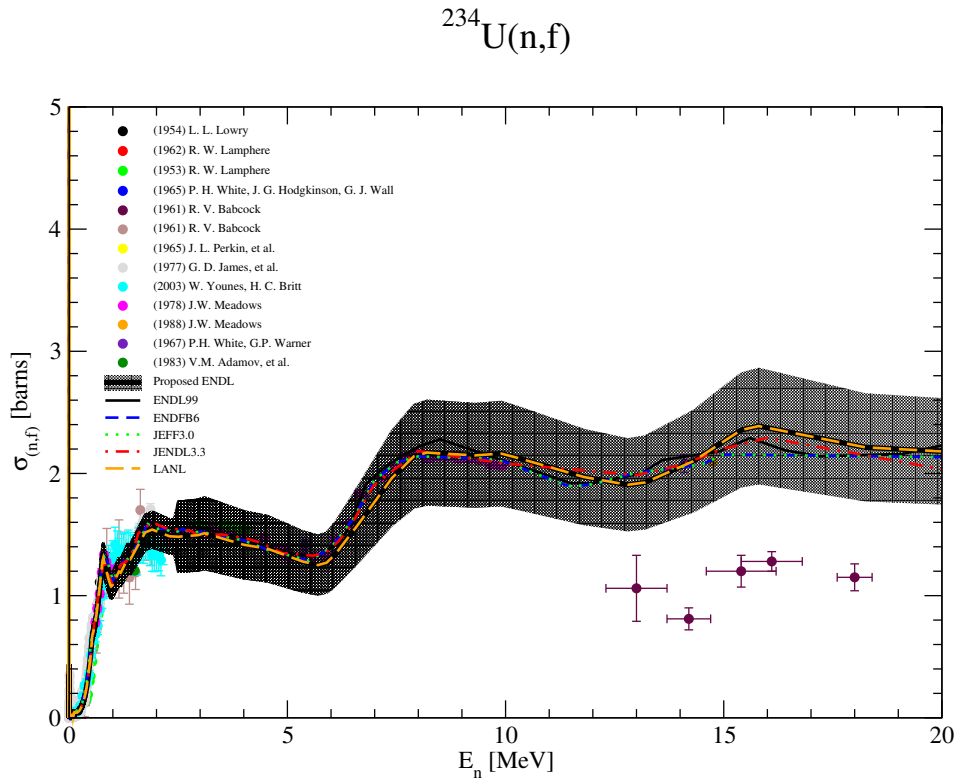

FIG. 14: The ^{234}U fission cross section on a linear scale.

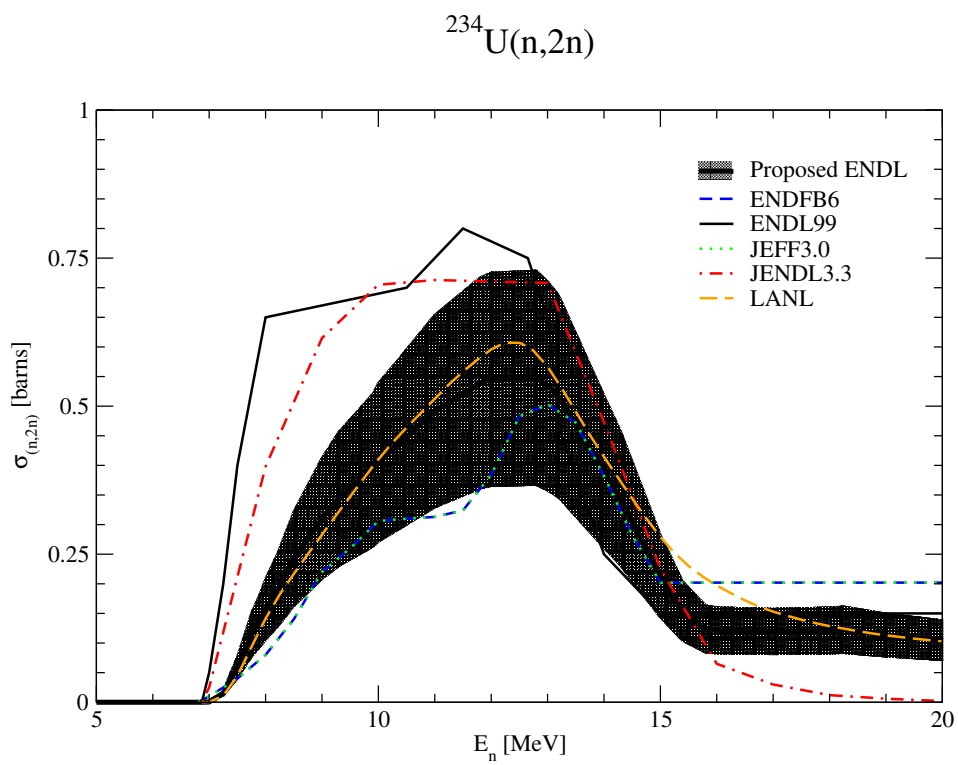

FIG. 15: The ^{234}U$(n, 2n)$ cross section.

Energy Range (MeV)	% Error Estimate		
	(n,γ)	(n,f)	$(n,2n)$
0.01-0.1	8.2	1.0	n/a
0.1-1.0	7.0	1.0	n/a
1.0-5.32	9.8	1.0	n/a
5.32-20.0	9.8	1.0	6.6

TABLE V: Error estimates for reactions on the ^{235}U nucleus.

VI. ^{235}U

For this nucleus, we adopt a hybrid of several evaluations. We take the resonance region from the LANL evaluation, which is itself from a recent ORNL evaluation. Above the resonance region, we take the LANL capture and elastic cross sections. We adopt the fission cross section recently determined by R. White [19] and the $(n,2n)$ cross section from our own fitter code `da_fit`.

The LANL capture cross section is a hold over from an older ENDFB-VI evaluation, but it is much better agreement with the meager capture data than the existing ENDL99 evaluation. Furthermore, the evaluators folded in the structure from the fission cross section into the capture reaction. Since the ENDFB-VI evaluation is a fit to the capture data, our uncertainty is the average percent uncertainty of the available data over each energy range. For the range 0.01 - 0.1 MeV, we used data from Refs. [21–23]. For the range 0.1-1.0 MeV, we used data from Refs. [15, 23, 24]. Finally, for the range above 1.0 MeV, the capture cross section is dropping rapidly so we keep the uncertainties from the lower range as an estimate.

The LANL elastic scattering cross section is a result of subtracting the reaction cross sections computed with `gnash` from a generalized least-square fit of the total cross section. We include this reaction in this update to maintain consistency between the reactions.

R. White's fission is the result of a least-square fit to all available data on ^{235}U(n,f). His results are within uncertainties of both the LANL evaluation and the existing ENDFB-VI evaluation. He estimates an overall uncertainty of 1%.

For the $(n,2n)$ reaction, we performed our own generalized least-square fit to the existing cross section data using the `da_fit` fitting code. The results of our fitting are shown in Fig. 19. This fit includes all of the data sets shown in the plot and was strongly levered by the new GEANIE data reanalyzed in Ref. [20]. The uncertainty in Table V are output from this fit. In this fit, the cross section was constrained to go to zero at threshold and this explains why the uncertainty band shrinks as the cross section goes to zero. We comment that the new LANL evaluation is in excellent agreement with our fit.

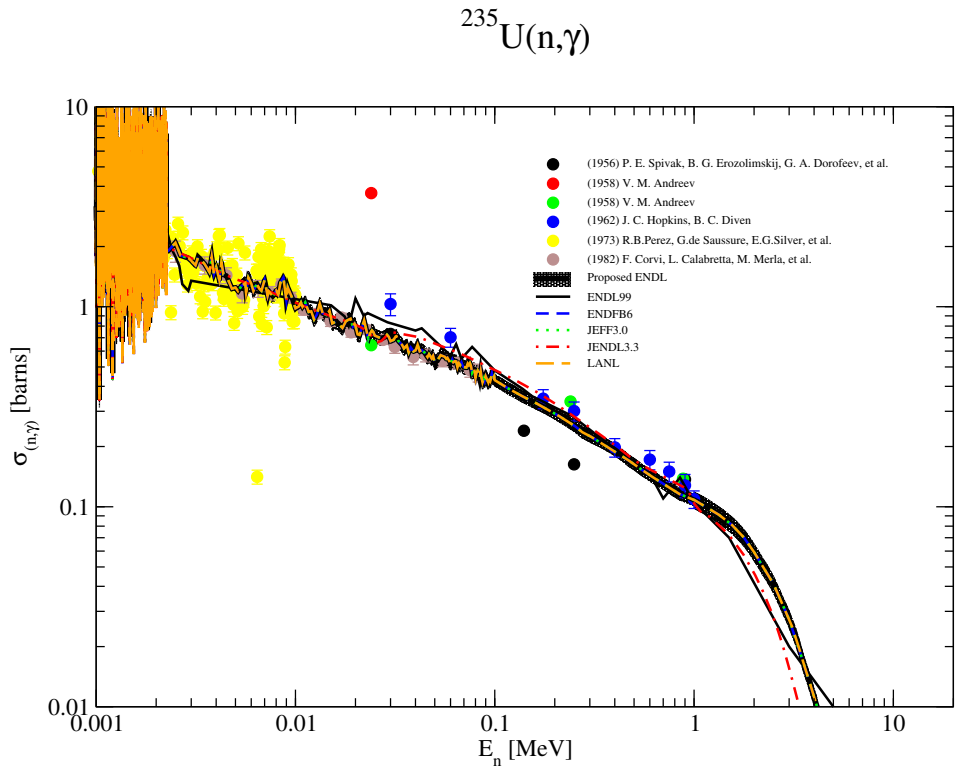

FIG. 16: The ^{235}U capture cross section.

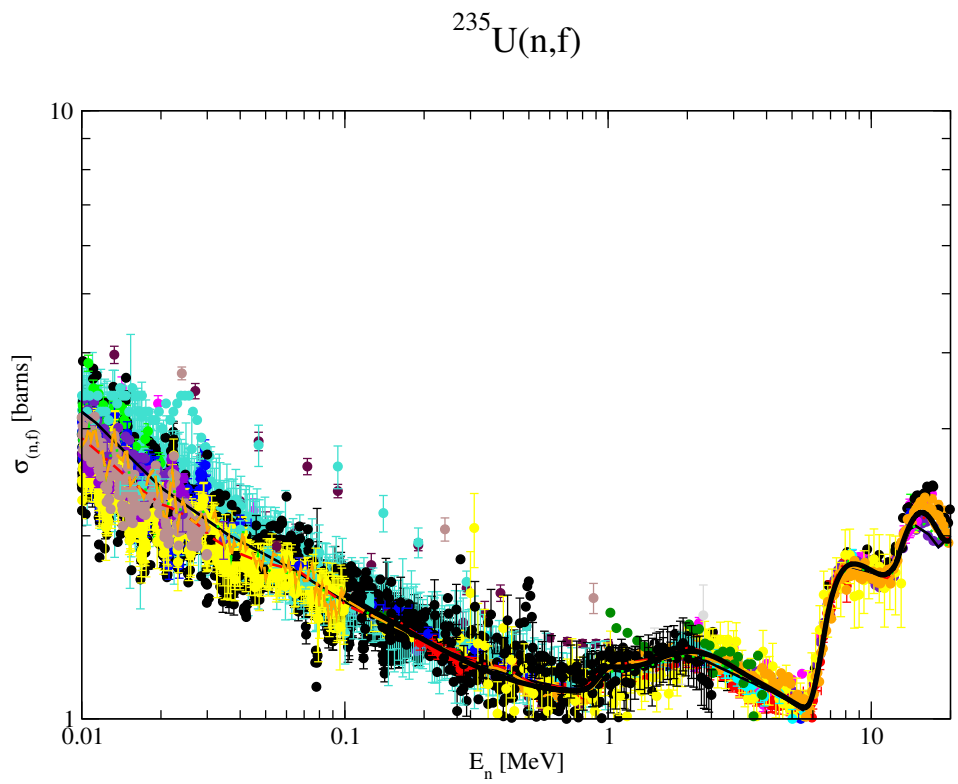

FIG. 17: The ^{235}U fission cross section on a logarithmic scale. Due to the large number of data sets we suppressed the legend in this plot.

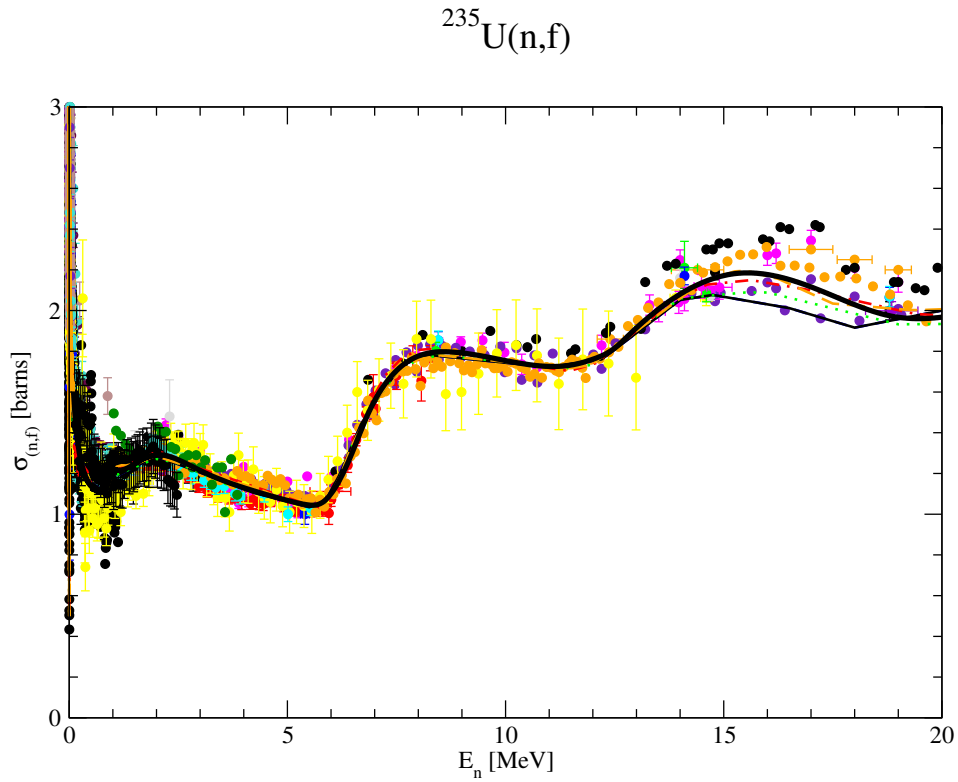

FIG. 18: The ^{235}U fission cross section on a linear scale. Due to the large number of data sets we suppressed the legend in this plot.

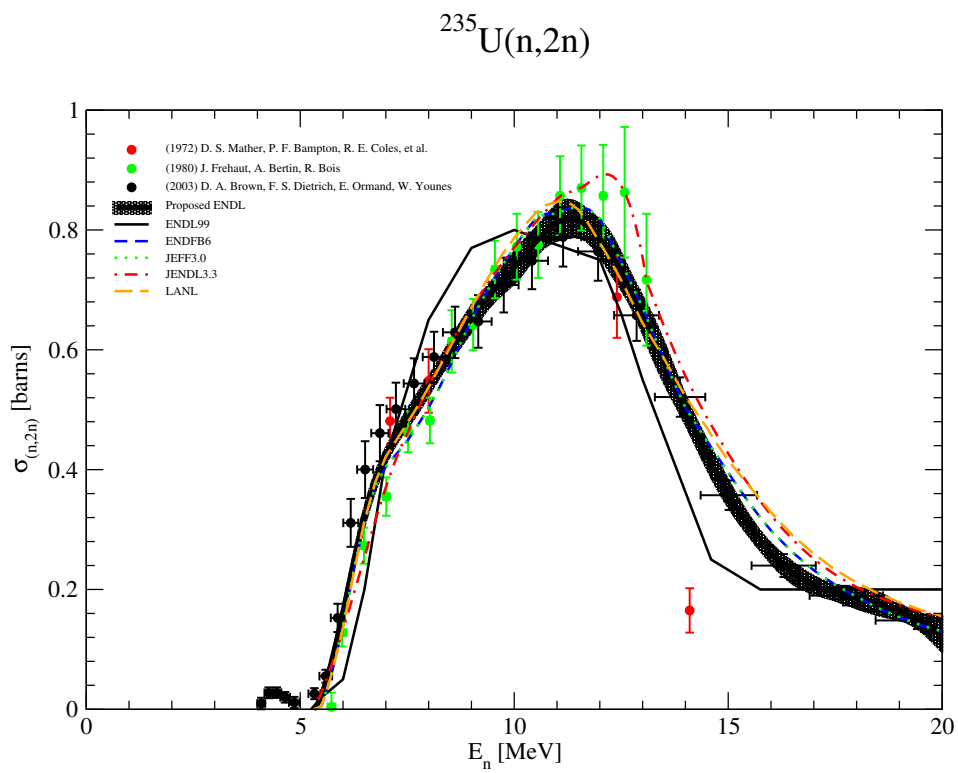

FIG. 19: The ^{235}U$(n, 2n)$ cross section.

Energy Range (MeV)	% Error Estimate		
	(n,γ)	(n,f)	$(n,2n)$
0.001-0.3	4.0	10	n/a
0.3-1.0	33	4.7	n/a
1.0-6.57	33	2.3	n/a
6.57-20.0	33	2.7	14

TABLE VI: Error estimates for reactions on the ^{236}U nucleus.

VII. ^{236}U

We adopt the new LANL evaluation in its entirety. Like the other LANL evaluations, this evaluation is a combination of `gnash` calculations, fits to measured cross section data, and resonance parameters from an earlier ENDFB-VI evaluation. There is enough data for both capture and fission to perform reasonable fits, even though the state of the data does require some discussion. Plots of this evaluation and all available nuclear data are shown in Figs. 20, 22, 21, and 23.

We take the LANL $(n,2n)$ cross section without modification. The `gnash` calculations were tuned so that both the capture and fission cross sections were reasonably reproduced, so that we can be assured that there is no competition problem with the calculated $(n,2n)$ cross section. As before, we compute the uncertainty on the LANL $(n,2n)$ cross section using Eq. (16).

For the fission cross section, we note that LANL performed generalized least-square fits to the data of Refs. [25–27]. All three data sets were ratio measurements of ^{236}U(n,f) to ^{235}U(n,f) cross sections since the many absolute cross section measurements differ significantly in their normalization. For the uncertainty, we compute the average percent error in the ratio measurements used in the fit and add in an additional 1.5% in quadrature to account for the uncertainty in the ^{235}U(n,f) cross section evaluation, which used a slightly older evaluation than we use here. The cross section from 1-100 keV is an extrapolation, so we use Eq.(16) to set the uncertainty here. We comment that this estimate does not cover the spread of the evaluations in this region. The uncertainties are tabulated in Table VI.

For the capture cross section, the LANL evaluators also performed a generalized least square fit. However, this analysis is tricky since the there are several disagreeing data sets in the 0.3 - 3 MeV region. In this region, we follow the LANL evaluation, but adopt a 33% uncertainty to account for the large spread in the data normalizations. In the 1 - 300 keV region, this evaluation is in excellent agreement with the data except at the low end where it transitions into the resonance region. Since the data sets begin to diverge here, we follow the LANL evaluation. For the uncertainty, we take the average percent uncertainty from the data.

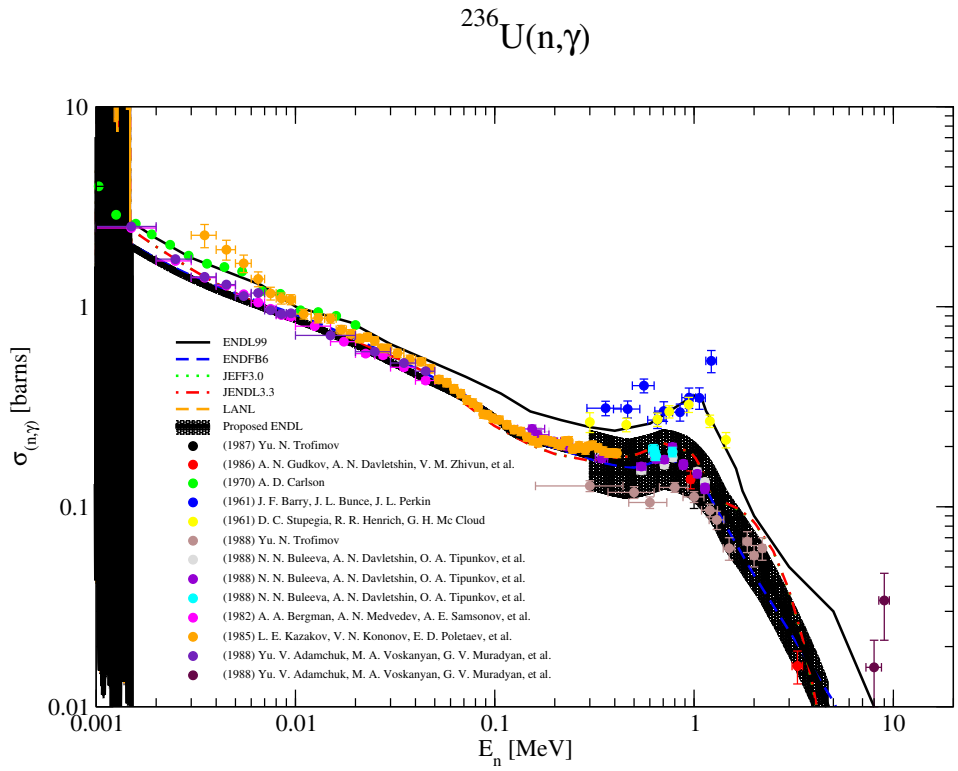

FIG. 20: The ^{236}U capture cross section.

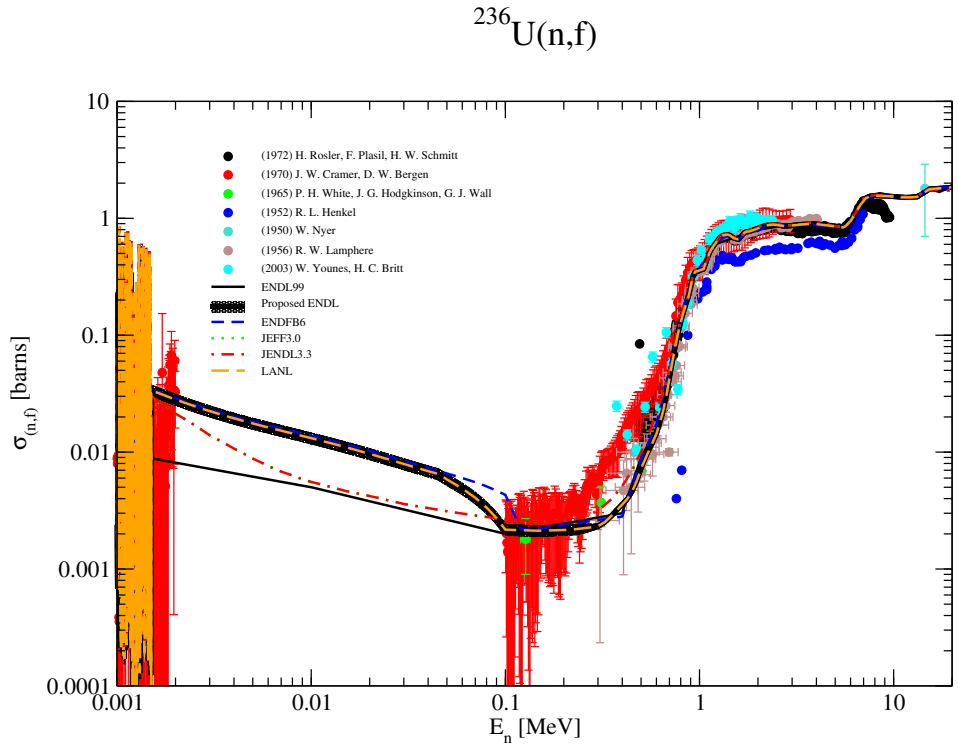

FIG. 21: The ^{236}U fission cross section on a logarithmic scale.

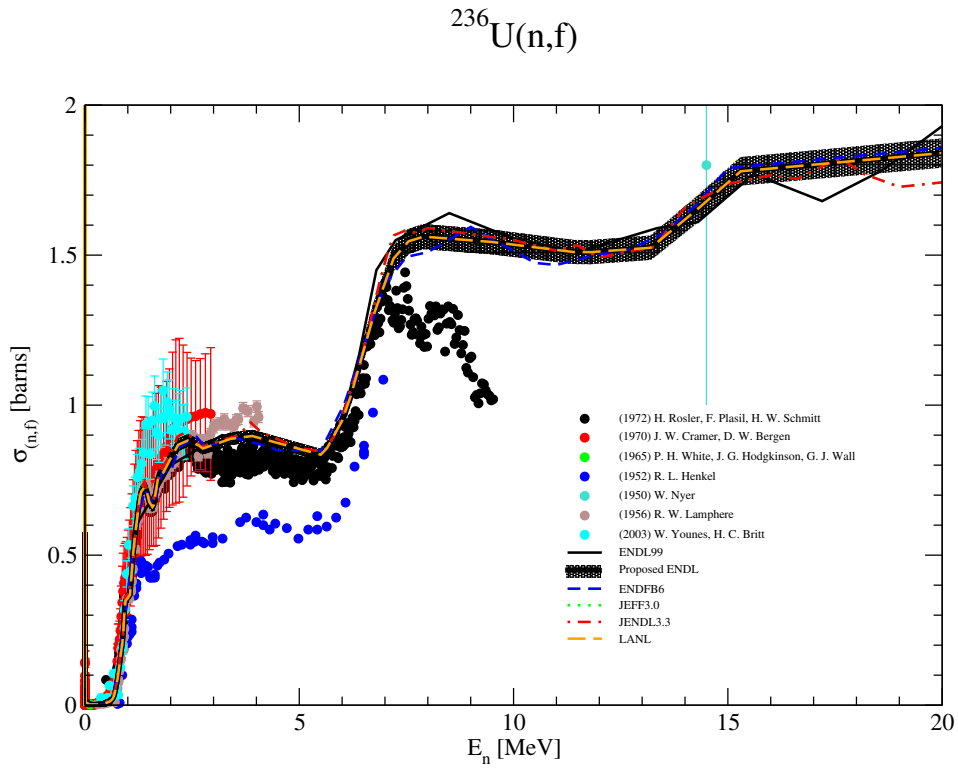

FIG. 22: The ^{236}U fission cross section on a linear scale.

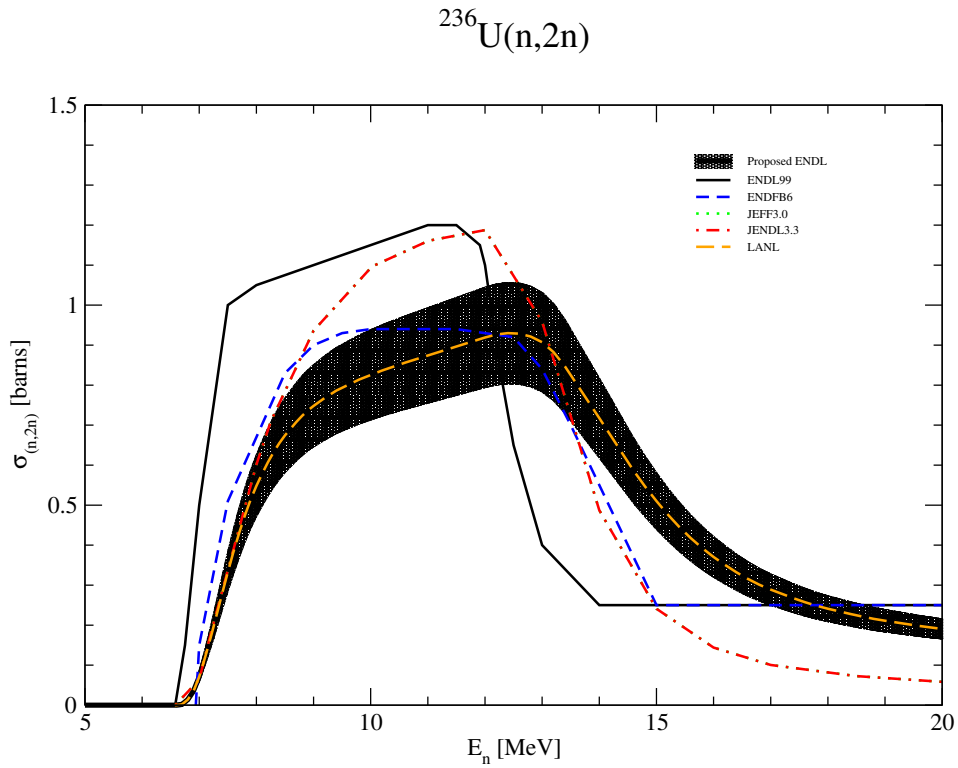

FIG. 23: The ^{236}U$(n, 2n)$ cross section.

VIII. ^{237}U

For this evaluation, we adopt a hybrid of the recent LANL evaluation [31], the recent (n, f) evaluation of Younes, Britt and Wilhelmy [32] which is based on ^{237}U(n, f)surrogate measurements, and the older ENDFB-VI evaluation for the resonance region.

In general, there is very little data on ^{237}U since it is unstable. In fact, there are only is one direct measurement for (n, f): the famous Pommard bomb-shot data [29]. There is also two points from Cowen *et al.* [30], based on LANL radiochemical work and the surrogate data from Younes *et al.*. As noted in [32], the Pommard bomb-shot data seem to have had a significant Np contamination which fouled the (n, f)measurement at higher energies. Because of this dearth of data, assessing uncertainties for reactions on this isotope is problematic.

For resonance region, we chose to adopt JENDL3.3 's evaluation because the evaluators fit a several of the resonances seen in the Pommard bomb-shot data above 45 eV. These data were unaffected by the Np contamination, so we believe it is sound. Below this fitted region, JENDL3.3 use an average picket fence spectrum. In the thermal region, JENDL3.3 agrees with accepted values for the resonance integrals and thermal cross sections.

For the fission cross section, we adopt the evaluation from Ref. [32]. In this evaluation, Younes *et al.*used surrogate (t, pf) data to extract the (n, f) cross section in the region from 0.5 - 2 MeV. They then used this measurement as the baseline first chance fission estimate. On top of this, they added second and third chance fission estimates from `gnash` calculations. They also provided an uncertainty estimate on the fission cross section in the range 0.5 - 2 MeV of 10%. Above this region, we assume a 20% uncertainty from a combination of their estimate of the modeling uncertainty and the extrapolation of the first chance fission cross section. This is shown in Table VII.

For the capture and $(n, 2n)$cross sections, we use the LANL evaluation above 10 keV and JENDL3.3 below 3 keV. In between these values, we use the ENDFB-VI evaluation to interpolate. We have faith that the LANL calculations are reasonable since they are based on the same systematic study used to pin down the OMP and gamma-ray strength function in the other uranium isotopes.

Since the LANL fission evaluation is a poor representation of the (limited) data, our replacement the fission cross section introduces the competition problem seen in the ^{232}U and ^{234}U evaluations. We performed the same rescaling in this isotope and saw a 20% increase in the $(n, 2n)$cross section and only a 50% reduction in the capture cross section. In both cases, the uncertainty was computed from Eqs. 16 and (19).

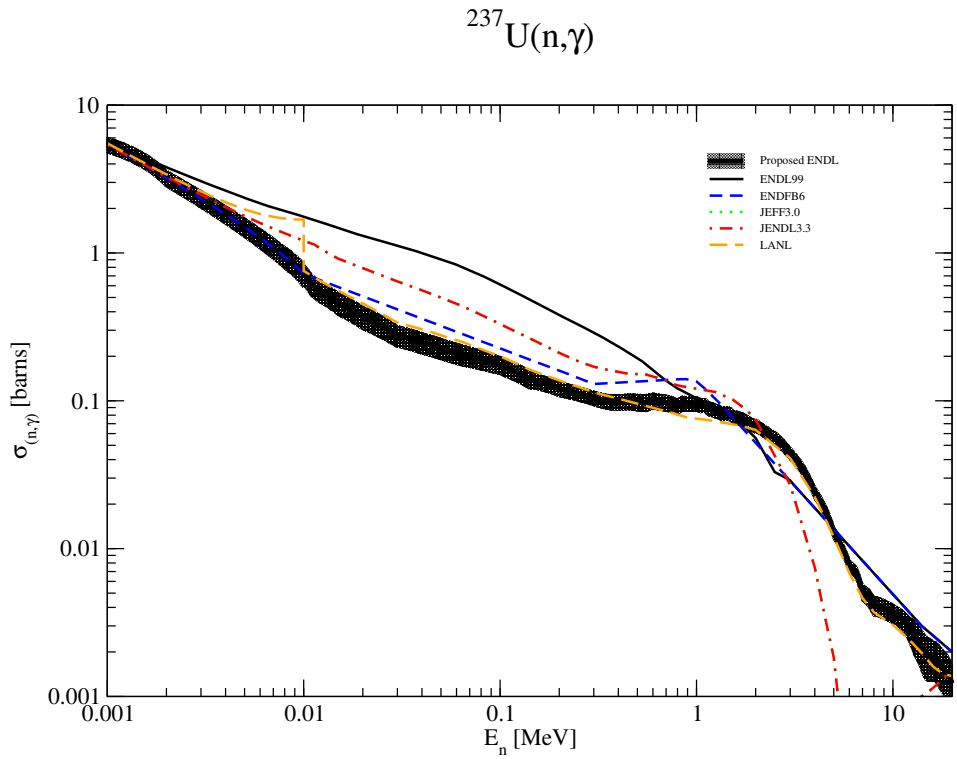

FIG. 24: The ^{237}U capture cross section.

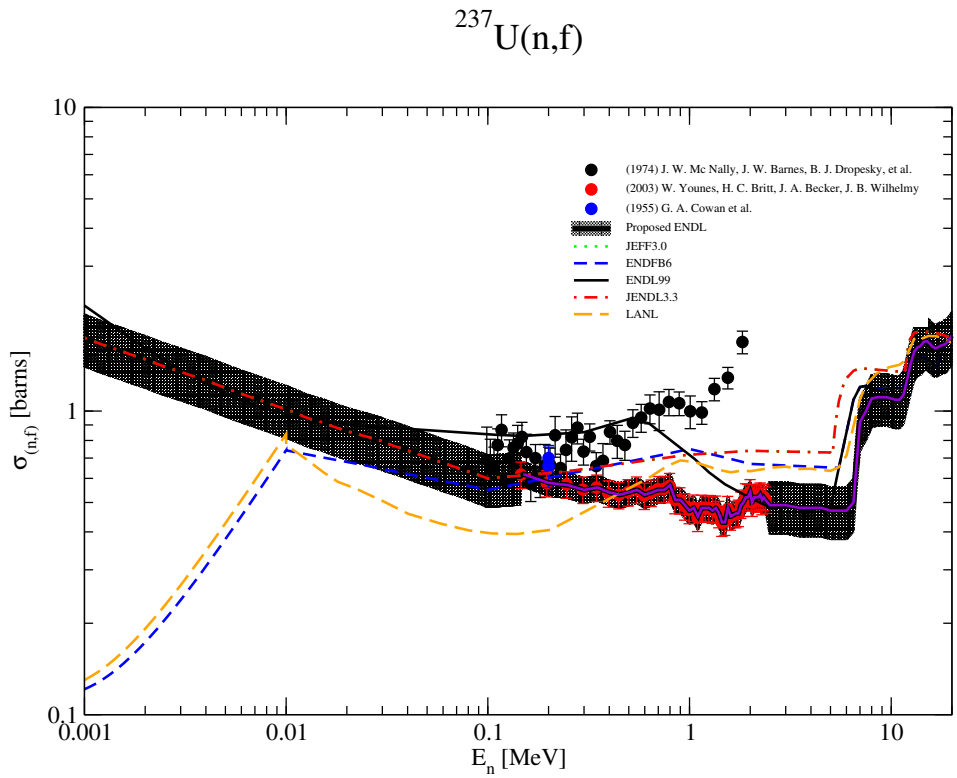

FIG. 25: The ^{237}U fission cross section on a logarithmic scale.

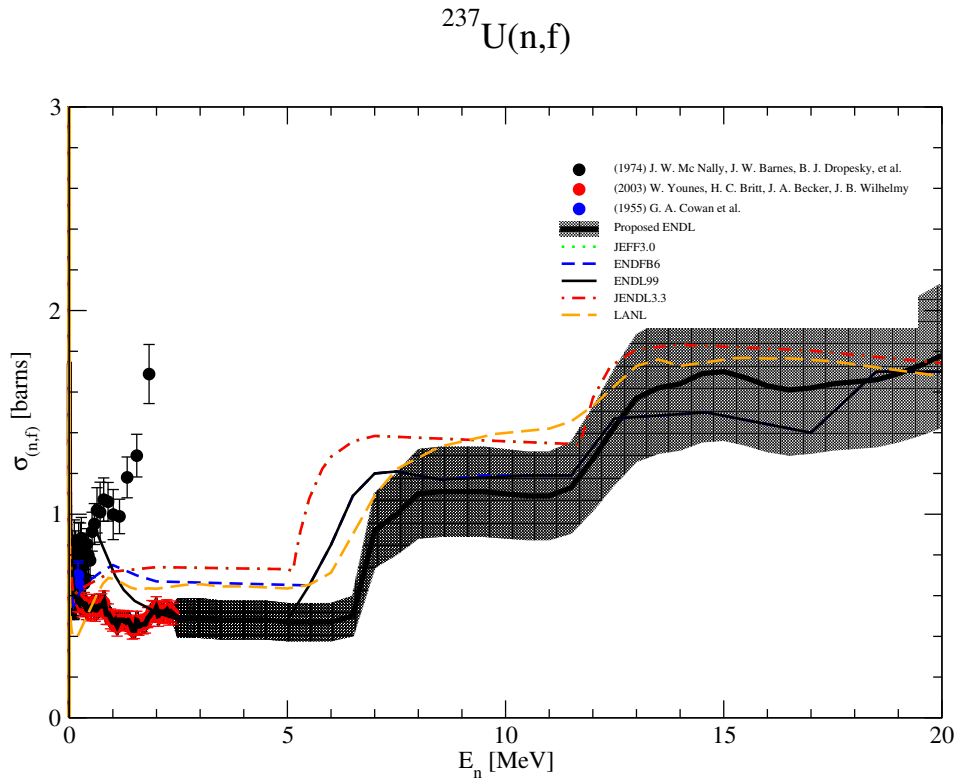

FIG. 26: The ^{237}U fission cross section on a linear scale.

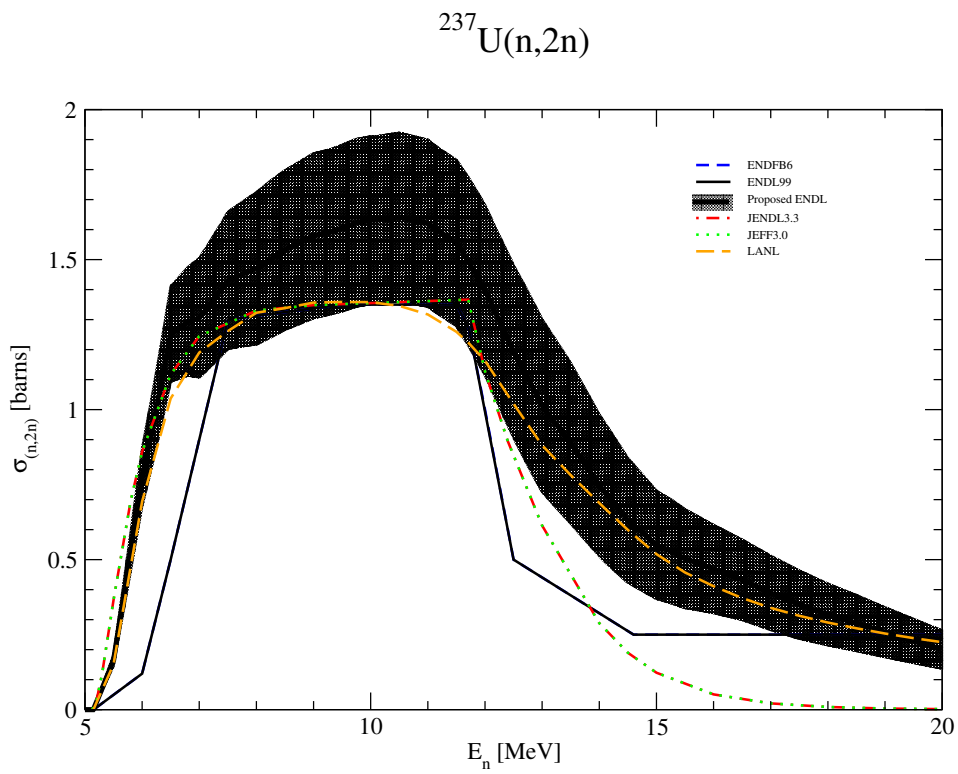

FIG. 27: The ^{237}U$(n, 2n)$ cross section.

Energy Range (MeV)	% Error Estimate		
	(n,γ)	(n,f)	$(n,2n)$
0.01-0.145	16	20	n/a
0.145-2.5	11	10	n/a
2.5-5.15	10	20	n/a
5.15-20.0	23	20	24

TABLE VII: Error estimates for reactions on the ^{237}U nucleus.

Energy Range (MeV)	% Error Estimate		
	(n,γ)	(n,f)	$(n,2n)$
0.01-1.0	1.0	1.0	n/a
1.0-6.18	1.0	0.95	n/a
6.18-20.0	1.0	0.97	5.63

TABLE VIII: Error estimates for reactions on the ^{238}U nucleus.

IX. ^{238}U

Our evaluation for this isotope is a hybrid of our fit to the $(n,2n)$ cross section and the recent fission and capture fits performed at JAERI [1, 8] and the existing ENDL99 evaluation. The JAERI fits are more recent than ENDFB-VI and more comprehensive than the recent LANL evaluations in that the JAERI fits performed simultaneous fits to both the absolute and ratio data simultaneously. For the uncertainty on the fission evaluation, we take it directly from Ref. [8].

For the capture, we use the JENDL3.3 evaluation below 1 MeV. Above this value, they use a reaction model, so instead we use the existing ENDL99 evaluation which is in good agreement with the data. We estimate the overall uncertainty to be 1% for entire cross section. This value is an estimate based on the uncertainties of the earlier fits in [33]. In principal the uncertainties can be extracted directly from the JENDL3.3 evaluated data file, but the `fete` translation code does not yet support covariances.

For the $(n,2n)$ reaction, we performed our own generalized least-square fit to the existing cross section data using the `da_fit` fitting code. The results of our fitting are shown in Fig. 30. This fit was difficult due to the discrepant data in the peak. JENDL3.3 chose to fit the lower sets while ENDFB-VI chose to fit the higher sets. We actually fit both leading to much smaller, but possibly unrealistic, uncertainties. In the next round of these evaluations we will reinvestigate the data sets in for this reaction in an effort to diagnose the discrepancy. In this fit, the cross section was constrained to go to zero at threshold with a slope at threshold of 0.10829 barns/MeV. This value was chosen to reproduce the slope of `gnash` Hauser-Feshbach calculations at threshold. The uncertainty in Table VIII are output from this fit.

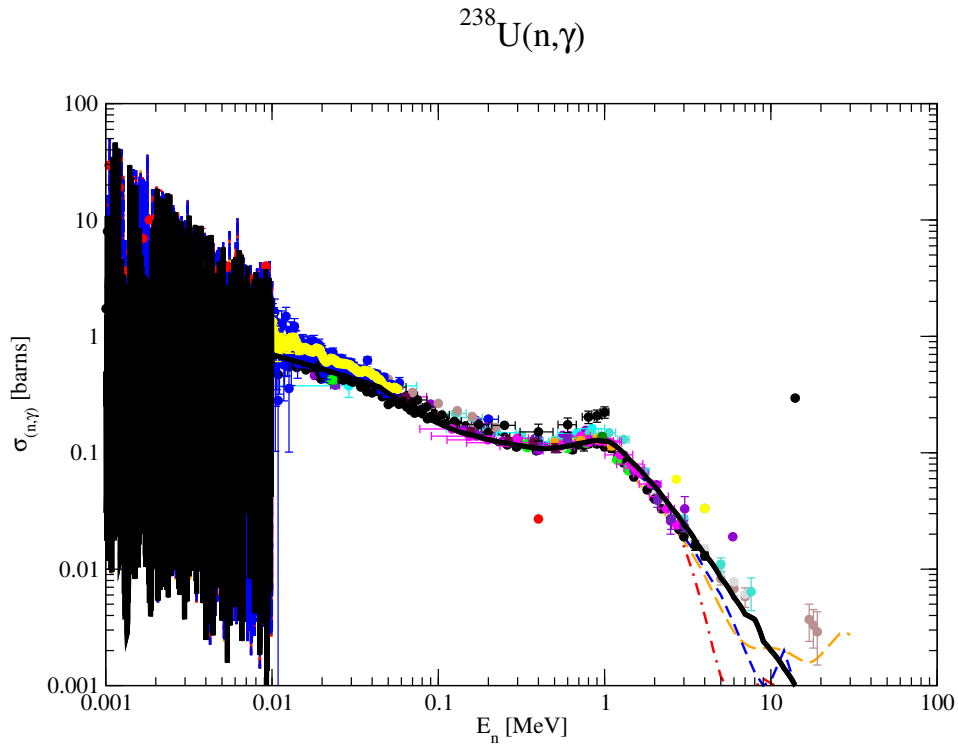

FIG. 28: The ^{238}U capture cross section. Due to the large number of data sets, we have suppressed the legend on this plot.

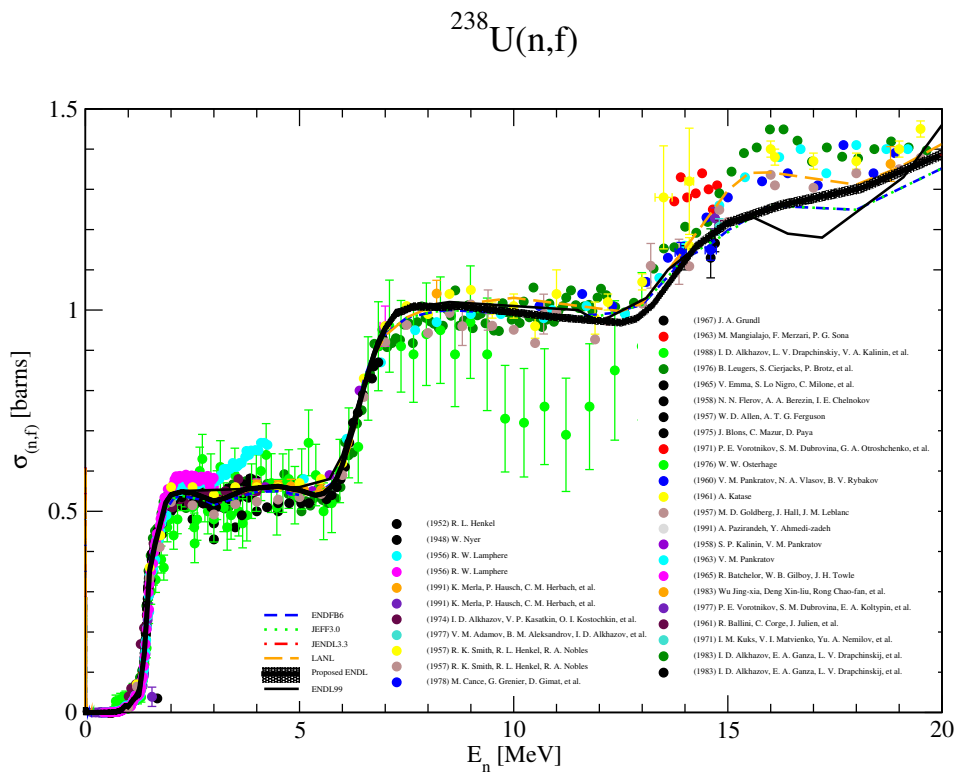

FIG. 29: The ^{238}U fission cross section.

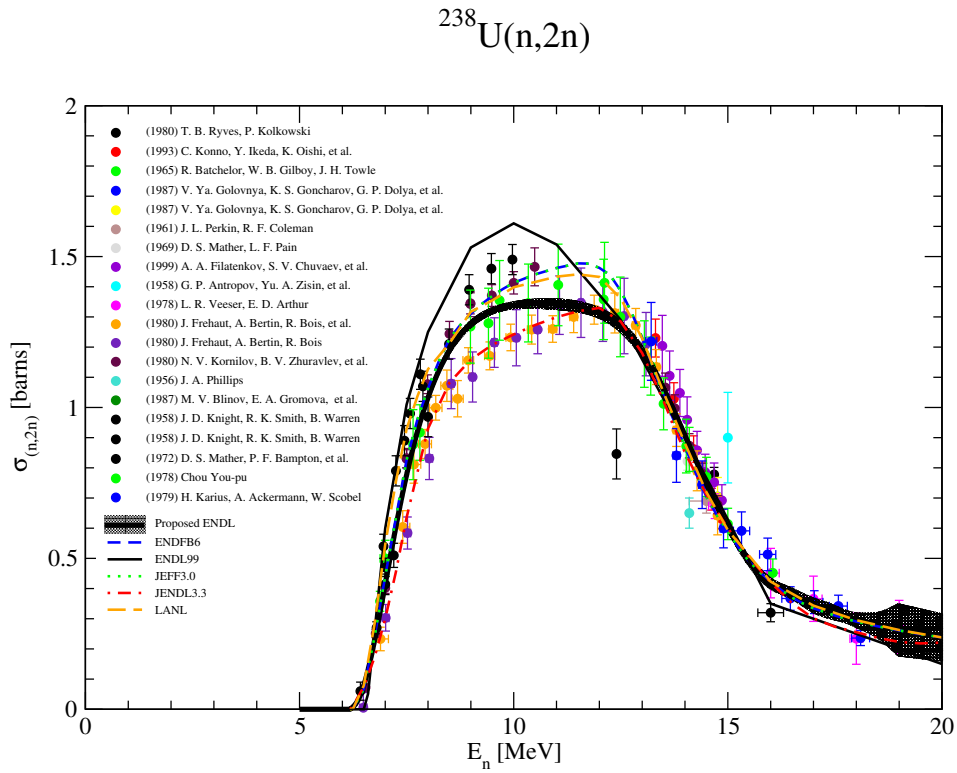

FIG. 30: The ^{238}U$(n, 2n)$ cross section.

X. ^{239}U

Our evaluation for this isotope is a hybrid of the existing ENDL99 evaluation, the new LANL evaluation, and our own fission cross section. There is only one high energy data set for reactions on this isotope, namely Ref. [32]. This surrogate data set only mocks up the first chance fission, so we must estimate the second and third chance fission somehow. To do this, we assume that the fission cross section from 30 keV - 2.6 MeV is solely due to first chance fission. Since it is relatively flat, we use the average of the cross section over this energy range as our estimate of the first chance fission cross section above 2.6 MeV. To produce the entire fission cross section, we then use the data from Ref. [32] from 30 keV - 2.6 MeV and above this, we use the LANL fission cross section after subtracting off our estimate of the LANL first chance fission and adding back in our estimate based on Ref. [32]. We adopt the uncertainty in Ref. [32] of 10% in the range 30 keV - 2.6 MeV and assess a modeling uncertainty using Eq. (16) resulting in an overall 33% uncertainty as shown in Table IX.

For the resonance region, we use a rescaled version of the LANL evaluation. The LANL evaluation has a "picket fence" spectrum of resonances for both the fission and capture cross sections, both based on the systematics of ^{237}U [31]. However the LANL evaluation fails to reproduce measured thermal cross sections. In fact, there

Energy Range (MeV)	% Error Estimate		
	(n,γ)	(n,f)	$(n,2n)$
0.001-0.03	33	33	n/a
0.03-2.6	33	10	n/a
2.6-4.827	33	33	n/a
4.827-20.0	33	33	33

TABLE IX: Error estimates for reactions on the ^{239}U nucleus.

were two measurements of the thermal fission cross section performed in the 1950's: Ref. [34] gives 14.9 ± 2.3 barns while Ref. [35] gives 12 barns, with no uncertainty, and give an upper limit of 20 barns. To compensate for this, we rescale the LANL thermal and resonance regions below 0.5 keV for fission and 0.1 keV for capture. Above these cut-offs, we interpolate onto our higher energy values.

For capture, elastic and $(n, 2n)$, we use the LANL evaluation above 0.1 keV since, as in previous evaluations, they used systematics to pin down the OMP and gamma-ray strength functions. Since the LANL evaluation uses a fission model which does not reproduce the (limited) data, all of the LANL cross sections must be rescaled to account for the differing competition as in ^{232}U and ^{234}U. As before, we assess a our modeling uncertainty on both the $(n, 2n)$ and capture cross section using Eq. (16),

correcting for the competition as in Eq. (19).

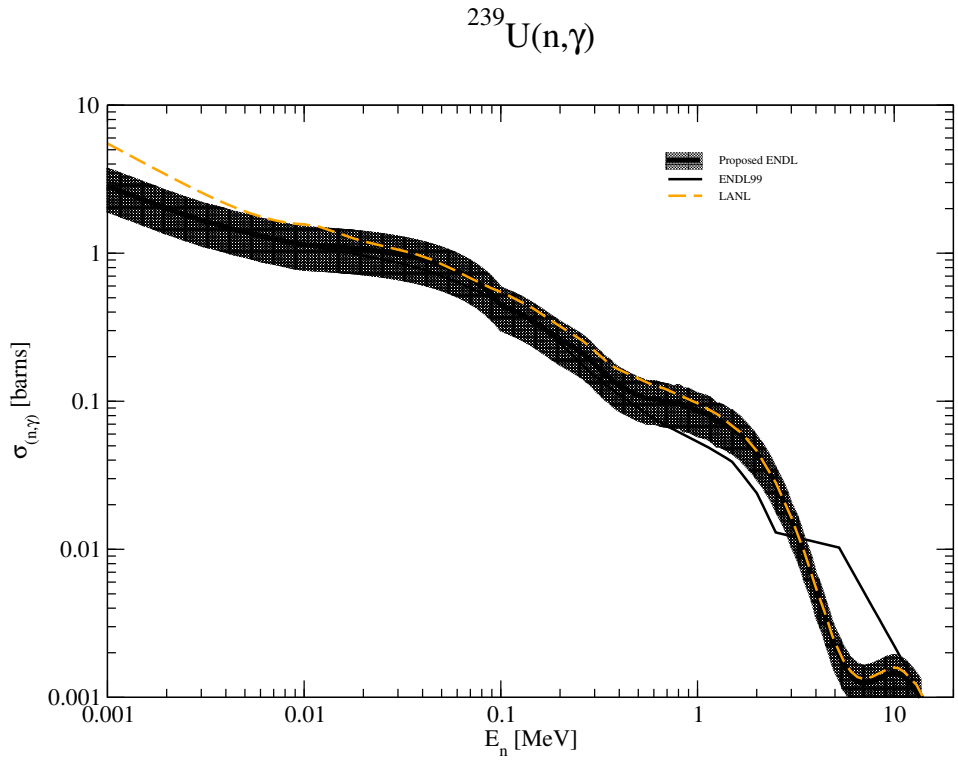

FIG. 31: The ^{239}U capture cross section.

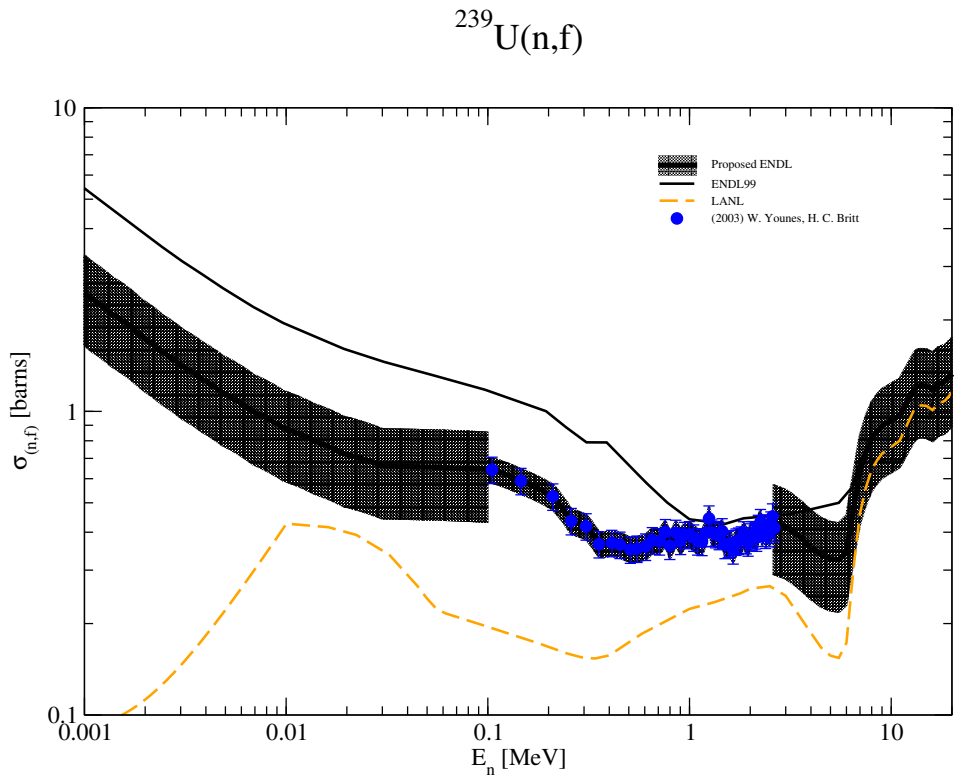

FIG. 32: The ^{239}U fission cross section on a logarithmic scale.

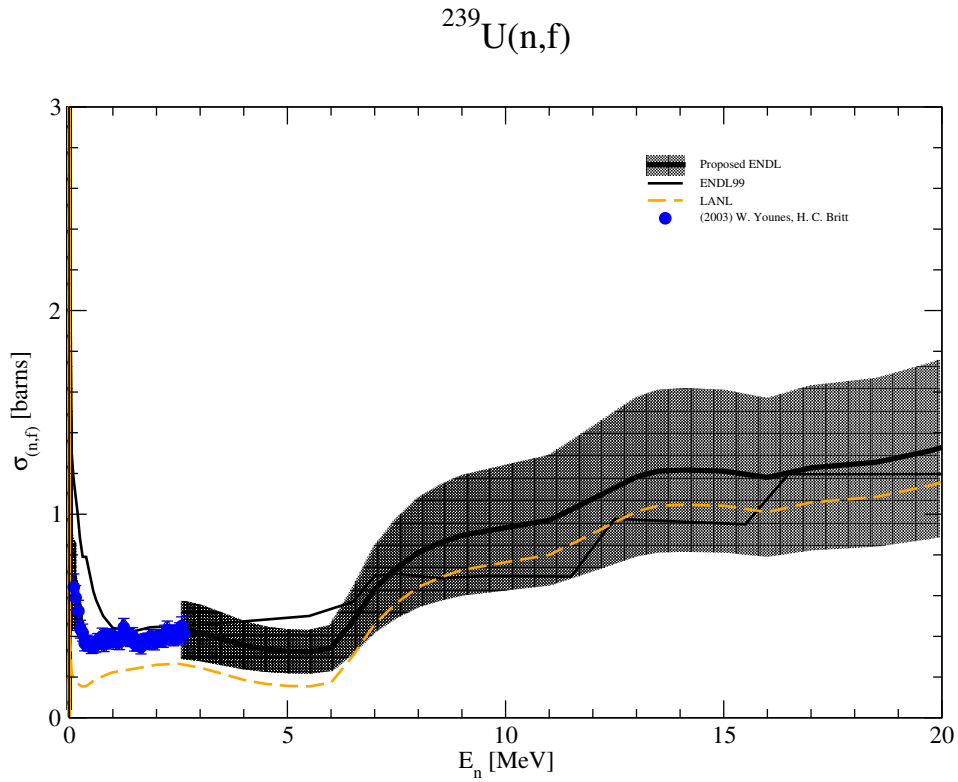

FIG. 33: The ^{239}U fission cross section on a linear scale.

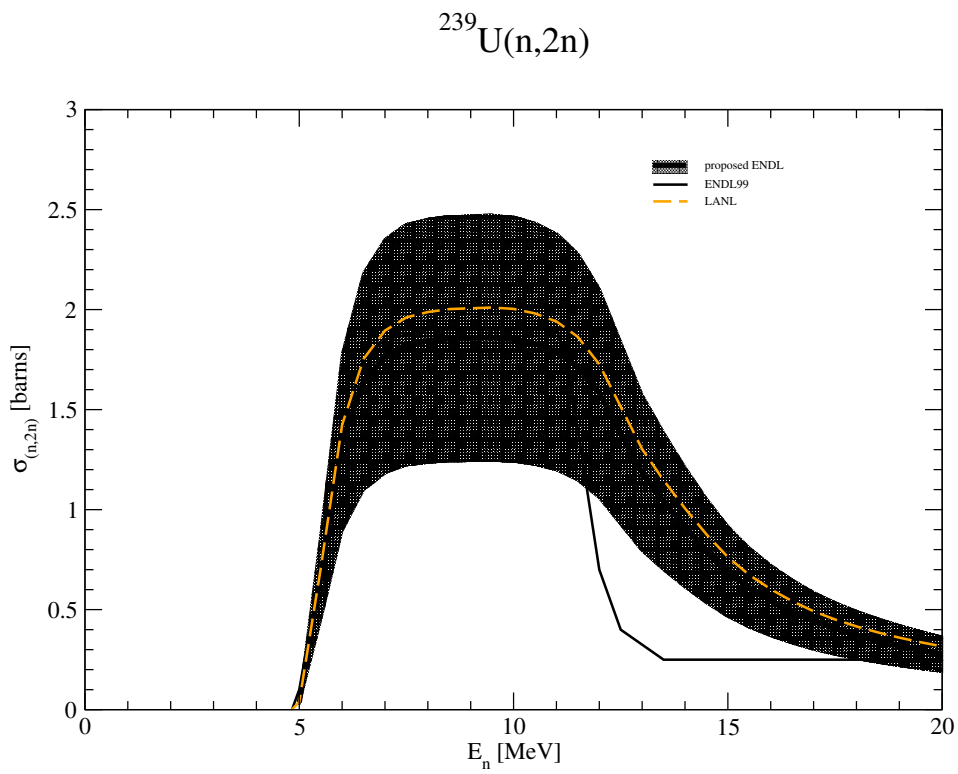

FIG. 34: The ^{239}U$(n, 2n)$ cross section.

XI. ^{240}U

Until the recent LANL evaluation, the only evaluation for reactions on ^{240}U was in the ENDL99 database. Now that there are two evaluations that differ so dramatically, we are in somewhat of a bind. There is no data to guide us in adopting either evaluation. Both evaluations come from systematics at some level. The LANL evaluation is smoother simply because it is the result of a `gnash` calculation. Our provisional solution is to produce two databases: one containing the original ENDL99 evaluation and another containing the LANL evaluation. In either case, our modeling uncertainty estimates from Eq. (16) gives 33% for all of the cross sections over the entire energy range.

XII. ^{241}U

This nucleus is not present in any database and is a recent addition for ENDFB-VII from LANL. It is based on a combination of resonances from n+^{237}U and `gnash` calculations. Since there is no data nor any any other evaluations to compare against, there is no way to judge the quality of this evaluation aside from examining the calculations themselves. This is difficult since the `gnash` calculations are necessarily based on incomplete nuclear structure information and optical model calculations using an OMP fit to nuclear reactions on nuclei much closer to the valley of stability. We simply adopt the LANL evaluation as is. In any event, our modeling uncertainty estimates from Eq. (16) gives 33% for all of the cross sections over the entire energy range.

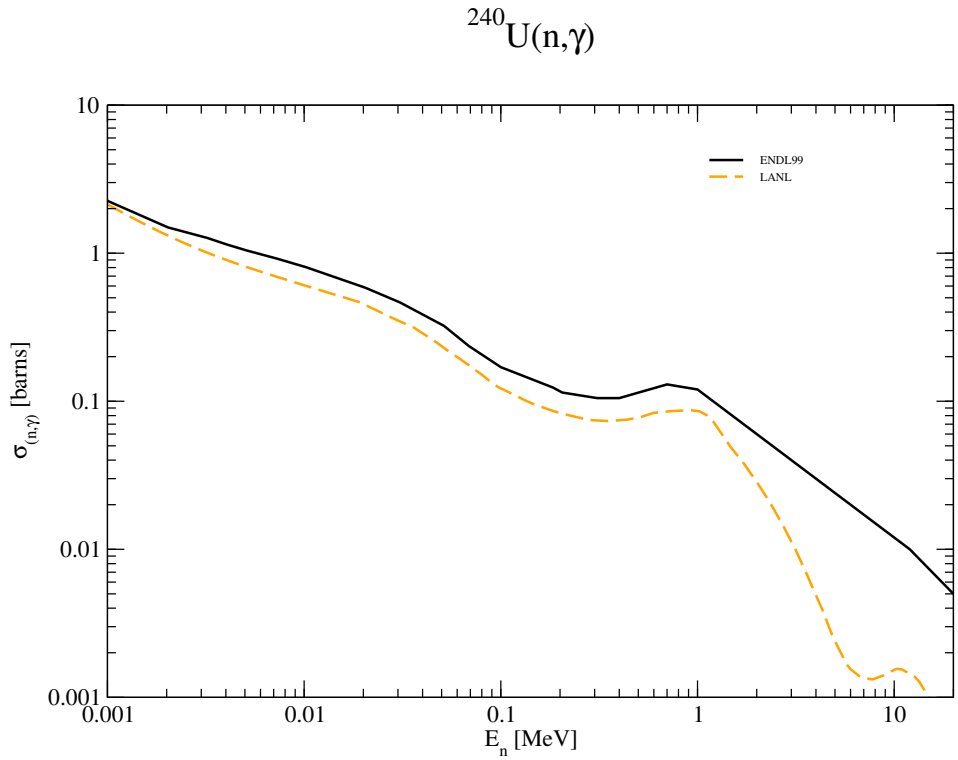

FIG. 35: The ^{240}U capture cross section.

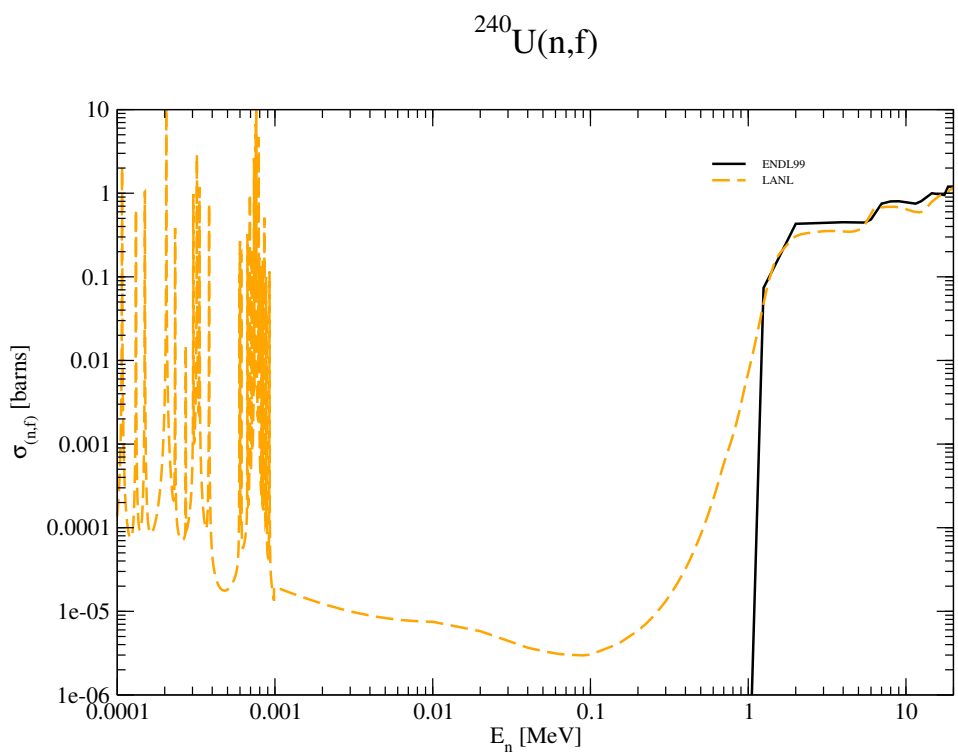

FIG. 36: The ^{240}U fission cross section on a logarithmic scale.

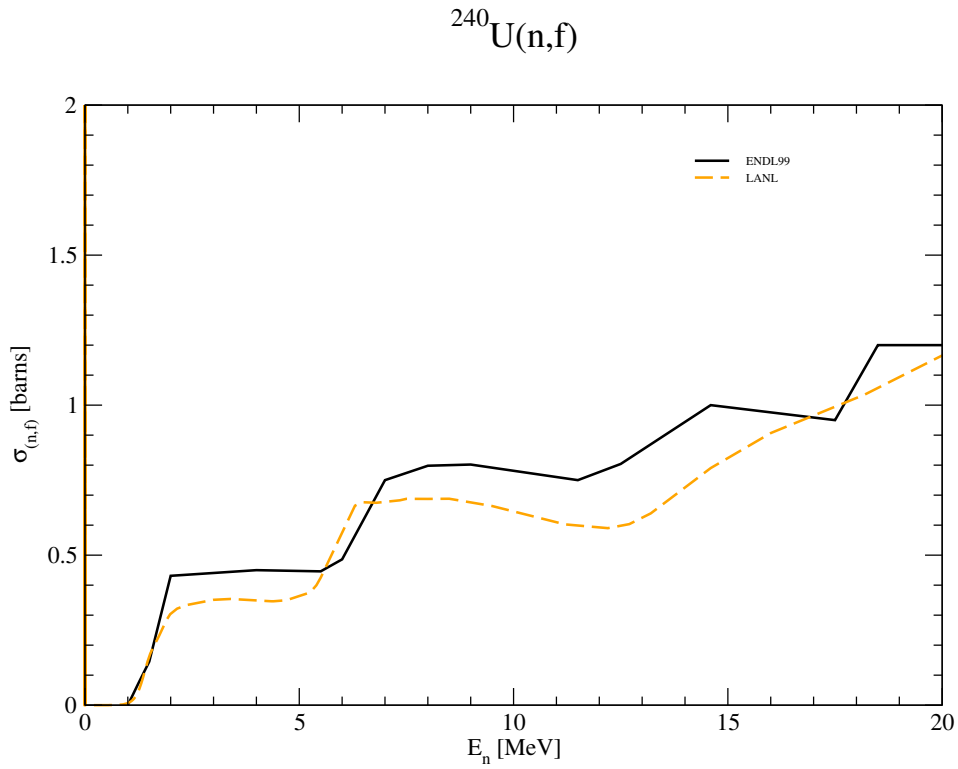

FIG. 37: The ^{240}U fission cross section on a linear scale.

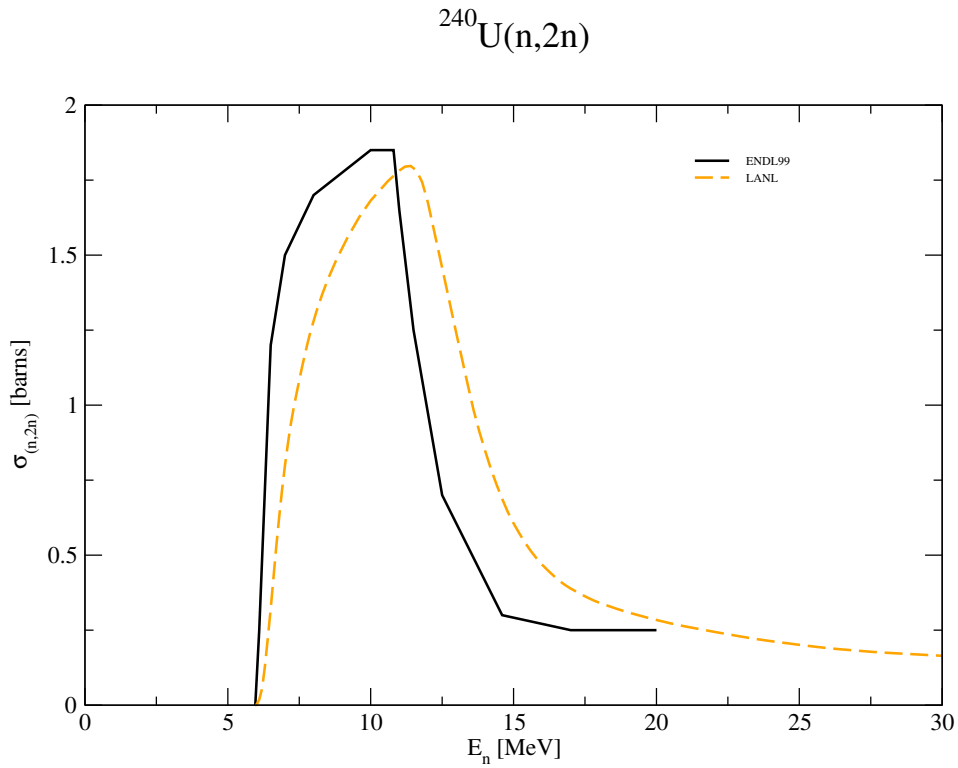

FIG. 38: The ^{240}U$(n, 2n)$ cross section.

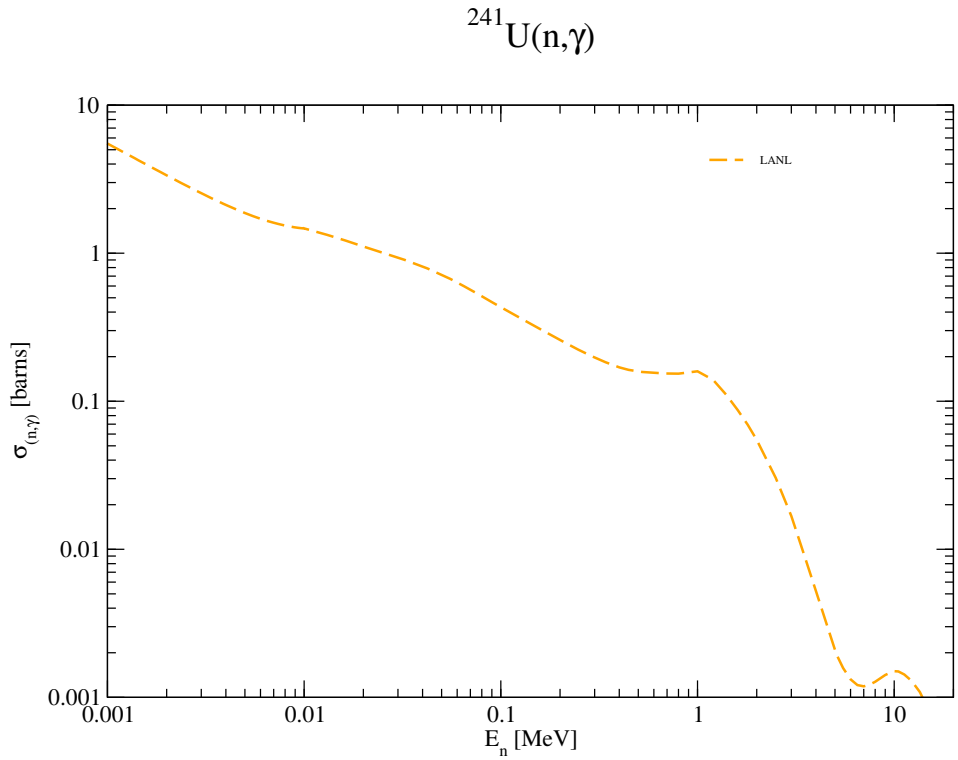

FIG. 39: The ^{241}U capture cross section.

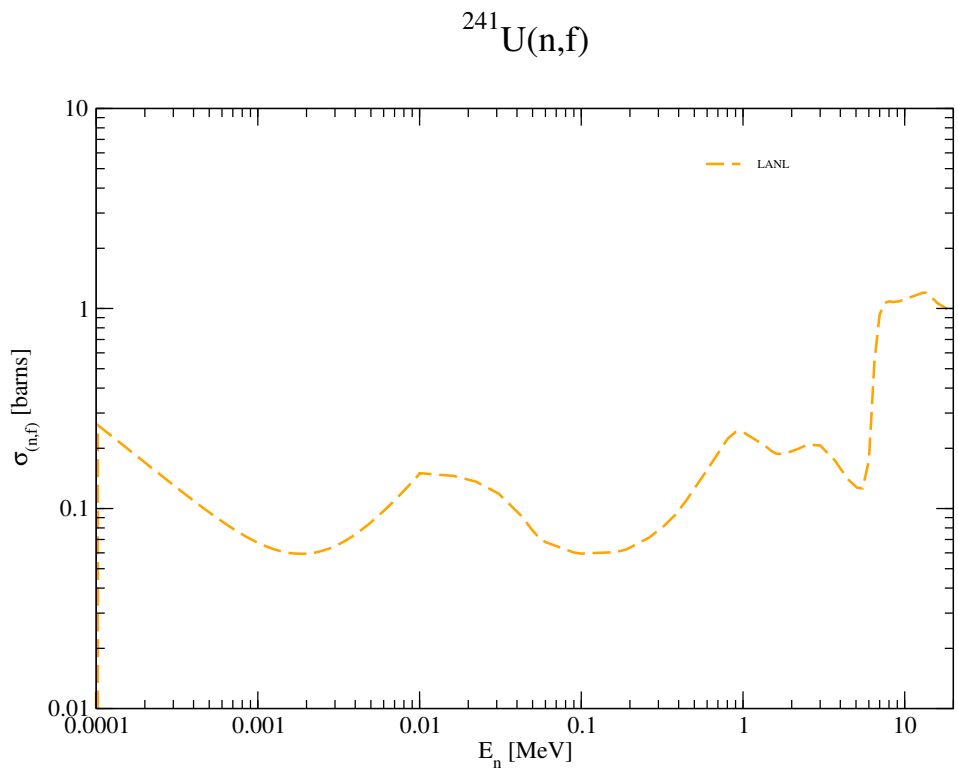

FIG. 40: The ^{241}U fission cross section on a logarithmic scale.

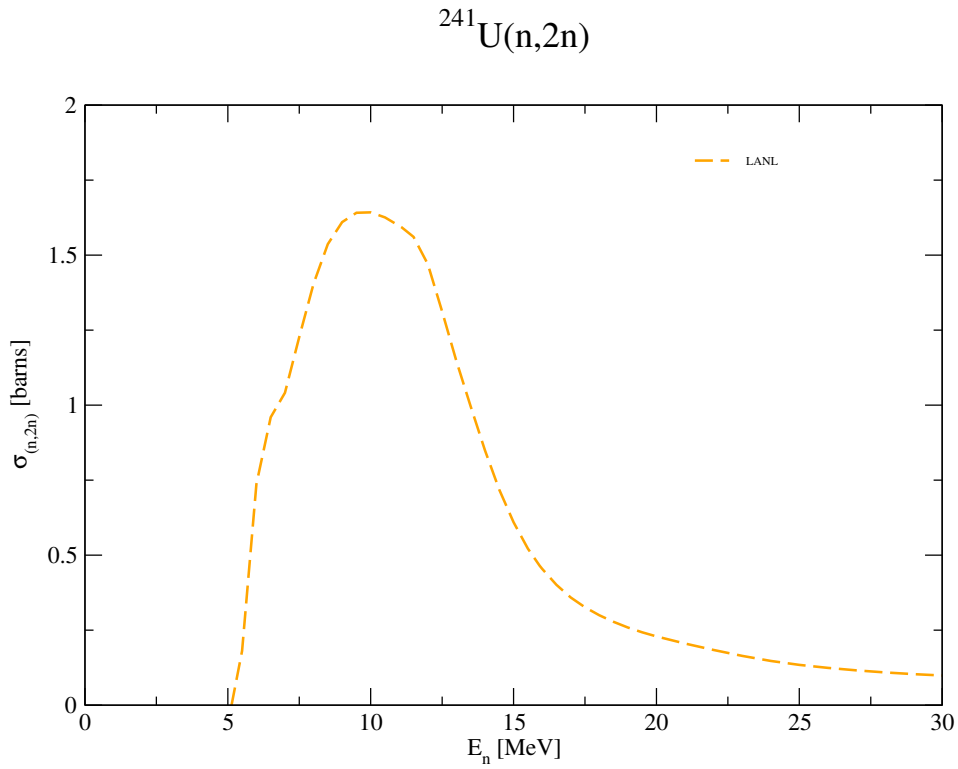

FIG. 41: The ^{241}U$(n, 2n)$ cross section.

XIII. CONCLUSIONS & FUTURE PLANS

Re-evaluating and improving the evaluated databases is an on-going process: new experiments are performed all the time and the tools we use to analyze them become increasingly sophisticated. Nevertheless, this pass at updating the uranium isotopes should result in a significant improvement in our understanding of radiochemical diagnostics.

Acknowledgments

The authors wish to thank Frank Dietrich and John Anderson for their help in the analysis performed here.

This work was performed under the auspices of the U.S. Department of Energy by University of California, Lawrence Livermore National Laboratory under Contract W-7405-Eng-48.

[1] K. Shibata, *et al.*, "Japanese Evaluated Nuclear Data Library Version 3 Revision-3: JENDL-3.3," J. Nucl. Sci. Technol. **39**, 1125 (2002); K. Shibata, "Descriptive Data of JENDL-3.3 (Part I and II)," JAERI-Data/Code 2002-026 (2003).
[2] Preliminary ENDF/B-VII Library, `http://www.nndc.bnl.gov/csewg_members/eval/`.
[3] D. Brown, F. Dietrich, T. Hill and D. McNabb "Updated ENDL99 cross sections for U(n, γ) and U(n, f)," UCRL-ID-148410, Lawrence Livermore National Laboratory, (2002).
[4] B. Beck, `fudge` Manual, in preparation.
[5] D. Brown, G. Hedstrom, T. Hill, `fete` Manual, in preparation.
[6] D. Brown, `da_fit`Manual, in preparation.
[7] R.J. Howerton and M.H. MacGregor "The LLL Evaluated Nuclear Data Library (ENDL): Description of Individual Evaluations for Z=0-98," Lawrence Livermore National Laboratory Report UCRL-50400 Vol. 15 (1978).
[8] T. Kawano *et al.*, "Evaluation of Fission Cross Sections and Covariances for ^{233}U, ^{235}U, ^{238}U, ^{239}Pu, ^{240}Pu, and ^{241}Pu," JAERI-Research 2000-004 (2000).
[9] P.G. Young, *et al.*"Analysis of Neutron Reactions on ^{232}U and ^{234}U: Analysis and Evaluation" LA-UR-03-3205 (2003).
[10] S.F. Mughabghab, *Neutron Cross Sections*, Vol. 1, Part B, Academic Press (1984).
[11] P. Young, private communication.
[12] Farrell, Los Alamos Report LA-4420 (1970).
[13] B.I.Fursov, E.JU.Baranov, M.P.Klemyshev, *et al.*, Atomnaya Energiya **61**: 383 (1986).

[14] P.G. Young, *et al.*"Analysis of Neutron Reactions on ^{233}U," LA-UR-03-1617 (2003).
[15] J.C. Hopkins, B.C. Diven, Nuclear Science and Engineering **12**: 169 (1962).
[16] L.W. Weston, R. Gwin, G. De Saussure, *et al.*Nuclear Science and Engineering **42**: 143 (1970).
[17] G.D. James, *et al.*, Phys. Rev. C **15**: 2083 (1977).
[18] G.V. Nuradyan, *et al.*, "Measurements of Neutron Capture Cross Sections of ^{234}U and ^{236}U," JINR-E3-98-212, 287 (1999).
[19] R. White, private communication.
[20] D. Brown, F. Dietrich, E. Ormand, W. Younes "^{239}Pu$(n,2n)^{238}$Pu and ^{235}U$(n,2n)^{234}$U Cross sections Inferred from `stapre` Calculations and GEANIE Measurements," in preparation.
[21] R.B. Perez, G. de Saussure, E.G. Silver, R.W. Ingle, H. Weaver, Nucl. Sci. Eng. **52** 46 (1973).
[22] V.N. Kononov, E.D. Poletaev, Ju.S. Prokopets, *et al.*, Atomnaya Energiya **38**, 81 (1975).
[23] F. Corvi, L. Calabretta, M. Merla, *et al.*. OECD Nuclear Energy Agency (NEA) Report NEANDC(E)-232, (3), 5 (1982).
[24] V.M. Andreev, Atomnaya Energiya **4**, 185 (1958); Soviet Atomic Energy **4**, 247 (1958); Journ. Nucl. En. **9**, 151 (1959).
[25] J.W. Behrens and G.W. Carlson, Nucl. Sci. Eng. **63**, 250 (1977).
[26] J. Meadows, Nucl. Sci. Eng. **65**, 171 (1978).
[27] J. Meadows, Ann. Nucl. En. **15**, 421 (1988).
[28] N.N. Buleeva, A.N. Davletshin, O.A. Tipunkov, *et al.*, Atomnaya Energiya **65**, 348 (1988).
[29] J.H. McNally, *et al.*, Phys. Rev. C **9**, 717 (1974).
[30] G.A. Cowan *et al.*, Los Alamos Scientific Laboratory Report No. LA-1669, (1955).
[31] P.G. Young and M.B. Chadwick, "Unstable Uranium Isotope Analysis," LANL T-16 Memo T-16:NW-2/10-00, (2000).
[32] W. Younes, H.C. Britt, J.B. Wilhelmy, "The ^{237}U(n,f) Cross Section," UCRL-ID-152621, Lawrence Livermore National Laboratory, (2003); W. Younes, H.C. Britt, "Simulated neutron-induced fission cross section for various Pu, U, and Th isotopes," submitted to Phys. Rev. C, UCRL-JC-153292; W. Younes, H.C. Britt, Phys Rev. C **67**: 024610 (2003).
[33] W. Poenitz, E. Pennington, A.B. Smith, and R. Howerton, "Evaluated Fast Neutron Cross Sections of Uranium-238," Argonne National Laboratory Report ANL/NDM-32 (1977).
[34] W.W.T. Crane, G.H. Higgins, R.W. Hoff, *et al.*, "Thermal neutron fission cross sections of ^{239}U and ^{233}Th," Lawrence Livermore National Laboratory Report UCRL-4728 (1956).
[35] P.R. Fields, G.L. Pyle, W.C. Bentley, Nucl. Sci. Eng. **2**, 33-37 (1957).